

Electronic Supplementary Information

High hole mobility in room temperature discotic liquid crystalline tetrathienoanthracenes

Indu Bala,^a Joydip De,^a Santosh Prasad Gupta,^b Harpreet Singh,^a Upendra Kumar Pandey^{*c,d} and Santanu Kumar Pal^{*a}

^aDepartment of Chemical Sciences, Indian Institute of Science Education and Research (IISER) Mohali, Sector-81, SAS Nagar, Knowledge City, Manauli-140306, India

^bDepartment of Physics, Patna University, Patna-800005, India

^cInterdisciplinary Centre for Energy Research (ICER), Indian Institute of Science (IISc) Bangalore, C. V. Raman Road, Bangalore 560012, Karnataka, India

^dPresent Address: Department of Electrical Engineering, School of Engineering, Shiv Nadar University, Gautam Buddha Nagar, Uttar Pradesh- 201314, India

E-mail: skpal@iisermohali.ac.in, santanupal.20@gmail.com, upendra.pandey@snu.edu.in

Table of contents

1. Experimental section.....	S3
2. Synthesis and characterization details.....	S4-S12
3. NMR spectra.....	S13-S22
4. TGA data.....	S23
5. POM data.....	S23
6. DSC thermogram.....	S24
7. X-ray diffraction data.....	S24-S28
8. Photophysical, Electrochemical and Theoretical studies.....	S29-S30
9. SCLC measurements.....	S31-S34
10. References.....	S34-S35

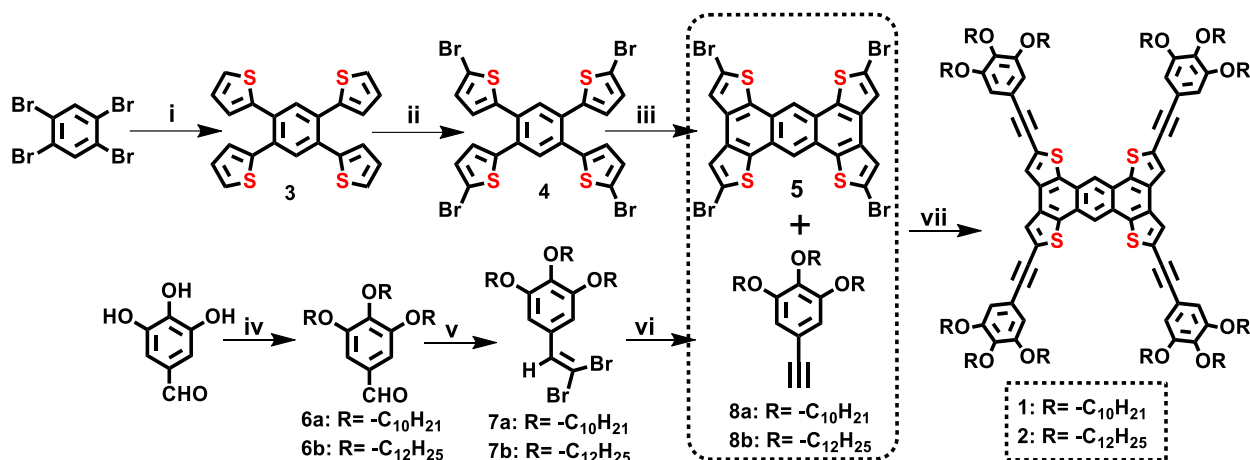
1. Experimental Section:

1.1 Materials and reagents: The chemicals available commercially were used as obtained. 3,4,5-trihydroxybenzaldehyde monohydrate, 1-bromodecane, 1-bromododecane, 1,2,4,5-tetrabromobenzene, 2-(tributylstannyl)thiophene, Bis(triphenylphosphine)palladium(II) dichloride ($\text{Pd}(\text{PPh}_3)_2\text{Cl}_2$), N-Bromosuccinimide (NBS), Iron(III) chloride (FeCl_3), Potassium carbonate (K_2CO_3), Tetrabromomethane (CBr_4), Triphenylphosphine (PPh_3), Tetrakis(triphenylphosphine)palladium(0) ($\text{Pd}(\text{PPh}_3)_4$), Copper Iodide (CuI), triethylamine (NEt_3) were all purchased from Sigma-Aldrich. Butyl Lithium (n-BuLi) was purchased from Avara Chemicals. The solvents: Nitromethane (CH_3NO_2), Chlorobenzene, Tetrahydrofuran (THF) and N,N-Dimethylformamide (DMF) used in synthesis were bought from Sigma-Aldrich. THF was dried in a lab by using benzophenone and sodium. Column chromatographic separations were done on silica gel (60-120) and neutral alumina gel. Alumina sheets pre-coated with silica gel (Merck, Kieselgel 60, F254) were implemented for thin layer chromatography (TLC).

1.2 Instrumentation: *The instrumental details for structural characterization (NMR, HRMS, FT-IR) thermal characterization (polarized optical Microscopy (POM), Thermogravimetric analysis (TGA), Differential scanning calorimetry (DSC), X-Ray diffraction (XRD)), photophysical studies (UV-Vis & Fluorescence), electrochemical characterization (Cyclic voltammetry) are similar to as mentioned in our previous papers and reproduced below for the reader's convenience.*¹⁻⁴

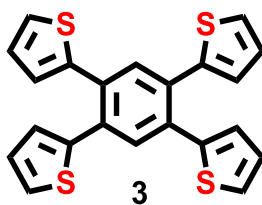
¹H NMR and ¹³C NMR (Bruker Biospin Switzerland Avance-iii 400 MHz and 100 MHz spectrometers, respectively), infrared spectroscopy (IR) (Perkin Elmer Spectrum Two). TGA experiments were scanned in temperature range 25 to 500 °C (Rate of heating: 10 °C min⁻¹) under nitrogen atmosphere on a Shimadzu DTG-60 instrument. Liquid crystalline textures were recorded with Nikon Eclipse LV100POL polarising microscope equipped with a Linkam heating stage (LTS 420). Q-imaging camera was used to capture the images. The phase transition temperatures and enthalpies associated to it were estimated by employing differential scanning calorimeter (Perkin Elmer DSC 8000 coupled to a controlled liquid nitrogen accessory (CLN 2)) with scan rate of 10 °C/min. X-ray diffraction (XRD) with instrument specification Cu K α ($\lambda=1.5418 \text{ \AA}$) as an X-ray source (GeniX 3D, Xenocs) operating at 50 kV and 0.6 mA. Two module Pilatus detector with 200 hybrid pixel from Dectris. UV-VIS-NIR spectrophotometer (Agilent Technologies UV-Vis-NIR Spectrophotometer), Fluorescence emission spectra were performed on Horiba Scientific Fluoromax spectrofluorometer 4. Cyclic Voltammetry (CV) studies were done using setup by Princeton Applied Research VersaSTAT 3. DFT calculations were performed with the use of Gaussian 09 suite of packages. A full optimization was carried out using the hybrid functional, Becke's three parameter exchange and the LYP Correlation Functional (B3LYP) at a split valence basis set 6-31G(d,p). For mobility measurement by space charge limited current (SCLC) method, effective cell thickness of SCLC cells were measured by using interferometry (Perkin Elmer lambda 35). Current –Voltage measurement and dielectric constant of the samples were obtained using Keithley 4200 SCS parametric analyzer.”

2. Synthesis and Characterization of intermediates and target compounds:



Scheme S1. (i) 2-(tributylstannyl)thiophene, PdCl₂(PPh₃)₂, DMF, 140 °C, 16h, 82 %; (ii) NBS, THF, RT, 16h, 80 %; (iii) FeCl₃, CH₃NO₂, Chlorobenzene, overnight, 78 %; (iv) RBr, K₂CO₃, DMF, 80 °C, 12h, 93 %; (v) CBr₄, PPh₃, dry DCM, 5 min, 80%; (vi) n-BuLi, dry THF, 24 h, 60 %; (vii) Pd(PPh₃)₄, CuI, NEt₃, DMF, 110 °C, 72h, 36 % for **1**, 32 % for **2**.

2.1 Synthesis of 1,2,4,5-tetra(thiophen-2-yl)benzene (3). The synthesis of the compound **3** has been reported elsewhere.⁵



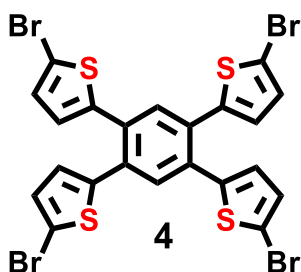
In a double neck round bottom flask (RBF), 30 ml dry DMF was taken and purged it with nitrogen for 15 minutes. To that, 1,2,4,5-tetrabromobenzene (1g, 2.54 mmol) was added followed by Pd(PPh₃)₂Cl₂ (126 mg, 0.18 mmol). After 5 minutes, 2-(tributylstannyl)thiophene (4.83g, 12.95 mmol) was dropwise added. The reaction was left to stir for 16 hours at 140 °C. After the completion of the reaction, extraction of reaction mixture with diethyl ether was done and then well dried using sodium sulfate. Column chromatographic using silica-gel as adsorbent and hexane-ethyl acetate as an eluent were done to get the white colored product in 82 % yield.

¹H NMR (400 MHz, CDCl₃, δ in ppm): δ 7.67 (s, 2H), 7.31-7.30 (dd, 4H, *J* = 4.96 Hz), 7.00-6.96 (m, 8H).

¹³C NMR (100 MHz, CDCl₃, δ in ppm): 141.74, 133.55, 133.40, 127.56, 127.18, 126.50.

FT-IR (cm^{-1}): 3100.10, 2929.00, 1738.00, 1661.90, 1593.40, 1544.00, 1532.50, 1481.36, 1441.52, 1422.20, 1376.50, 1262.40, 1237.84, 1201.50, 1079.70, 1053.00, 946.54, 900.95, 847.48, 835.20, 737.27, 702.98, 524.00.

2.2 Synthesis of 1,2,4,5-tetrakis(5-bromothiophen-2-yl)benzene (4). The synthesis of the compound **4** has been reported elsewhere.⁵



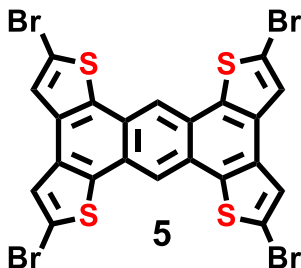
To a solution of compound **3** (1g, 2.46 mmol) in 20 ml dry THF, N-Bromosuccinimide (2.69g, 15.10 mmol) was added and reaction mixture was kept for stirring for 16 hours. After completing reaction, solvent was evaporated and the slurry was prepared in 60-120 mesh silica gel in order to purify it. The purification gives rise to white colored pure product in 80 % yield.

^1H NMR (400 MHz, CDCl_3 , δ in ppm): δ 7.50 (s, 2H), 6.97-6.96 (d, 4H, $J = 3.84$ Hz), 6.75-6.74 (d, 4H, $J = 3.80$ Hz).

^{13}C NMR (100 MHz, CDCl_3 , δ in ppm): 142.34, 133.28, 132.85, 130.29, 128.15, 113.74.

FT-IR (cm^{-1}): 3093.00, 2963.20, 2925.10, 2852.80, 1749.40, 1734.20, 1601.00, 1551.50, 1483.00, 1443.25, 1422.20, 1368.90, 1323.20, 1228.10, 1193.90, 1167.20, 1056.90, 1022.60, 976.27, 969.37, 931.32, 904.69, 866.64, 791.04, 737.27, 703.03, 661.17, 581.27, 528.00, 474.73.

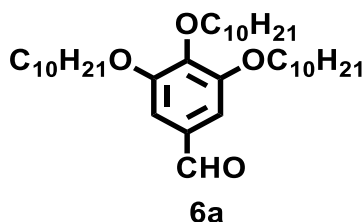
2.3 Synthesis of 2,5,9,12-tetrabromoanthra[1,2-*b*:4,3-*b'*:5,6-*b''*:8,7-*b'''*]tetrathiophene (5). The synthesis of the compound **5** has been reported elsewhere.⁵



To a solution of compound **4** (1.23g, 1.70 mmol) in warm chlorobenzene (60 ml), FeCl₃ (1.70g, 10.47 mmol) solution in 30 ml nitromethane was slowly poured (dropwise) for over 5 minutes. The reaction was kept for stirring at room temperature for overnight. The yellow colored solution was filtered and the filtered precipitates were allowed to stir with 10 % HCl/H₂O mixture for 30 minutes and washed with excess amount of methanol. The resultant mustard yellow precipitates were dried and quantitatively obtained in crude form with a yield of 78 %. The product was almost insoluble in all common inorganic solvents and hence limits its characterization by NMR Spectroscopy.

FT-IR (cm⁻¹): 2917.50, 2852.80, 1546.09, 1482.83, 1429.80, 1392.84, 1298.16, 12585.29, 1190.00, 1133.00, 973.18, 961.03, 858.80, 817.18, 803.29, 741.08, 615.51, 559.09, 494.19.

2.4 Synthesis of 3,4,5-tris(decyloxy)benzaldehyde (6a). The synthesis of the compound **6a** has been reported elsewhere.⁶



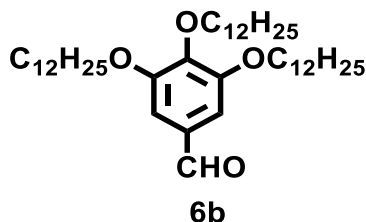
In a double neck RBF, dry DMF was purged with nitrogen for 15 minutes. Then, 3,4,5-trihydroxybenzaldehyde monohydrate (1g, 5.81 mmol) and K₂CO₃ (29.04 mmol, 4.01g) were stirred for 15 minutes. After that, the addition of 1-bromodecane (3.98g, 18.01 mmol) followed by a pinch of potassium iodide was done. The reaction was kept for stirring at 80 °C for 12 hours. The extraction with diethylether was performed and reaction mixture was evaporated and then purified by column chromatography. The purification enable to get the white colored product in 93 % yield.

¹H NMR (400 MHz, CDCl₃, δ in ppm): δ 9.83 (s, 1H), 7.08 (s, 2H), 4.07-4.01 (m, 6H), 1.83-1.71 (m, 6H), 1.49-1.44 (m, 6H), 1.35-1.27 (m, 36H), 0.89-0.86 (t, 9H, *J* = 6.84 Hz).

¹³C NMR (100 MHz, CDCl₃, δ in ppm): δ 191.44, 161.35, 153.66, 144.00, 131.58, 108.00, 73.78, 69.39, 64.28, 32.09, 32.06, 32.03, 30.49, 29.87, 29.81, 29.77, 29.73, 29.69, 29.65, 29.53, 29.50, 29.44, 29.41, 29.33, 28.66, 26.22, 26.18, 25.97, 22.84, 14.26.

FT-IR (cm⁻¹): 2955.50, 2923.88, 2854.09, 2723.40, 1697.85, 1585.80, 1497.97, 1468.45, 1440.90, 1381.47, 1331.43, 1228.20, 1148.20, 1116.95, 986.98, 825.84, 721.37, 653.56, 585.08.

2.5 Synthesis of 3,4,5-tris(dodecyloxy)benzaldehyde (6b). The synthesis of the compound **6b** has been reported elsewhere.⁶



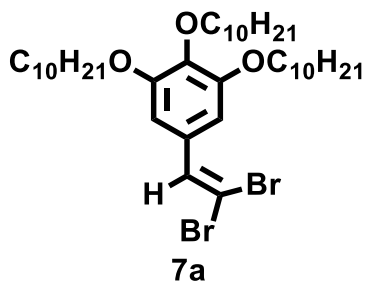
In a double neck RBF dry DMF was purged with nitrogen for 15 minutes. Then, 3,4,5-trihydroxybenzaldehyde (1g, 5.81 mmol) monohydrate and K₂CO₃ (29.05 mmol, 4.01g) were stirred for 15 minutes. After that the addition of 1-bromododecane (4.49g, 18.01 mmol) followed by a pinch of potassium iodide was done. The reaction was kept for stirring at 80 °C for 12 hours. The extraction with diethylether was performed and reaction mixture was evaporated and then purified by column chromatography. The purification enable to get the white colored product in 93 % yield.

¹H NMR (400 MHz, CDCl₃, δ in ppm): δ 9.83 (s, 1H), 7.08 (s, 2H), 4.07-4.01 (m, 6H), 1.83-1.73 (m, 6H), 1.49-1.45 (m, 6H), 1.30-1.26 (m, 48H), 0.89-0.86 (t, 9H, *J* = 6.84 Hz).

¹³C NMR (100 MHz, CDCl₃, δ in ppm): 191.42, 161.33, 153.66, 144.00, 131.58, 107.99, 73.78, 69.38, 64.27, 32.08, 30.49, 29.90, 29.87, 29.84, 29.81, 29.70, 29.64, 29.53, 29.52, 29.41, 29.33, 28.66, 26.22, 26.18, 25.96, 22.84, 14.26.

FT-IR (cm⁻¹): 2954.48, 2917.89, 2849.10, 2727.30, 1692.99, 1583.40, 1501.38, 1469.20, 1440.87, 1380.33, 1336.97, 1224.47, 1145.73, 1119.15, 1011.20, 988.40, 967.49, 823.53, 720.07, 649.76, 619.32.

2.6 Synthesis of 1,2,3-tris(decyloxy)-5-(2,2-dibromovinyl)benzene (7a). The synthesis of the compound **7a** has been reported elsewhere.⁷



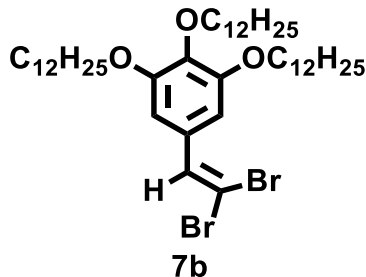
In one neck 100 ml RBF, compound **6a** (1g, 1.74 mmol) was taken in 15 ml dry DCM and cooled to 0 °C. To that, CBr₄ (1.15g, 3.48 mmol) was added for 10 minutes and the solution was allowed to stir. After 5 minutes, PPh₃ (1.59g, 6.08 mmol) was added and kept the solution to stir for another 5 minutes. After checking the TLC and on comparing it with reactant **6a**, the reaction was stopped. A new non-polar spot as compared to the reactant indicated the occurrence of reaction. Further the evaporation of the solvent for making slurry using silica-gel for column chromatography was done, giving rise to colourless liquid in 80 % yield.

¹H NMR (400 MHz, CDCl₃, δ in ppm): δ 7.37 (s, 1H), 6.77 (s, 2H), 3.99-3.94 (m, 6H), 1.81-1.72 (m, 6H), 1.48-1.43 (m, 6H), 1.34-1.27 (m, 36H), 0.90-0.87 (t, 9H, *J* = 6.86 Hz).

¹³C NMR (100 MHz, CDCl₃, δ in ppm): 153.01, 148.23, 138.84, 136.95, 130.14, 107.38, 88.20, 73.59, 69.35, 32.09, 32.06, 30.47, 29.88, 29.82, 29.79, 29.73, 29.65, 29.50, 26.23, 22.84, 14.26.

FT-IR (cm⁻¹): 2959.40, 2924.95, 2854.59, 1575.81, 1504.63, 1467.76, 1429.11, 1379.52, 1332.95, 1239.35, 1116.82, 835.85, 721.79, 684.00, 626.93.

2.7 Synthesis of 5-(2,2-dibromovinyl)-1,2,3-tris(dodecyloxy)benzene (7b). The synthesis of the compound **7b** has been reported elsewhere.⁷



In one neck 100 ml RBF, compound **6b** (1g, 1.52 mmol) was taken in 15 ml dry DCM and cooled to 0 °C. To that, CBr₄ (1.01g, 3.03 mmol) was added for 10 minutes and the solution was allowed

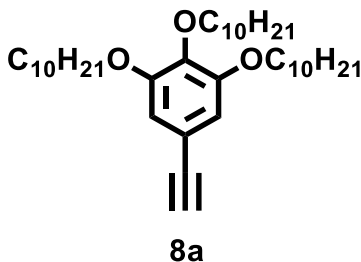
to stir. After 5 minutes, PPh_3 (1.59g, 6.08 mmol) added and kept the solution to stir for another 5 minutes. After checking the TLC and on comparing it with reactant **6b**, the reaction was stopped. A new non-polar spot as compared to the reactant indicated the occurrence of reaction. Further the evaporation of the solvent for making slurry using silica-gel for column chromatography was done, giving rise to colourless liquid in 80 % yield.

^1H NMR (400 MHz, CDCl_3 , δ in ppm): δ 7.37 (s, 1H), 6.76 (s, 2H), 3.98-3.94 (m, 6H), 1.81-1.71 (m, 6H), 1.48-1.31 (m, 6H), 1.34-1.26 (m, 48H), 0.90-0.86 (t, 9H, $J = 6.84$ Hz).

^{13}C NMR (100 MHz, CDCl_3 , δ in ppm): 153.01, 148.23, 138.85, 136.95, 130.13, 107.38, 88.20, 73.58, 69.34, 32.08, 30.47, 29.89, 29.85, 29.81, 29.79, 29.74, 29.56, 29.52, 29.49, 26.24, 22.84, 14.26.

FT-IR (cm^{-1}): 2955.50, 2921.64, 2851.79, 1575.11, 1506.05, 1467.99, 1430.21, 1379.66, 1335.51, 1244.09, 1123.20, 1015.00, 992.78, 868.65, 831.67, 809.87, 721.04, 680.40, 623.30.

2.8 Synthesis of 1,2,3-tris(decyloxy)-5-ethynylbenzene (8a). The synthesis of the compound **8a** has been reported elsewhere.⁷



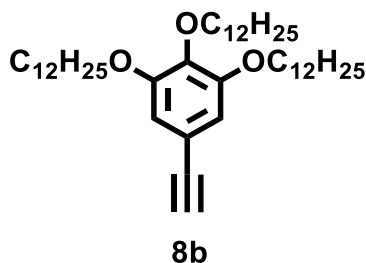
In a Schenk flask, addition of *n*-BuLi to a solution of **7a** (2.30g, 3.15 mmol) in dry THF under N_2 atmosphere, *n*-BuLi (1.6M in hexane)(7.87 mmol, 4.9 ml) in dry THF was carried out at -78 °C in a slow manner. Then the reaction was stirred for 24 hours at room temperature. After checking the TLC, the reaction was stopped and quenched with saturated NH_4Cl solution. After extraction with DCM, the organic layer was dried and evaporated to dryness and further subjected to purification. The purification by column chromatography using hexane-ethyl acetate as an eluent leads to obtain the product in 60 % yield as a colourless liquid.

^1H NMR (400 MHz, CDCl_3 , δ in ppm): δ 6.69 (s, 2H), 3.97-3.93 (m, 6H), 2.99 (s, 1H) 1.81-1.71 (m, 6H), 1.45-1.41 (m, 6H), 1.30-1.27 (m, 36H), 0.90-0.86 (t, 9H, $J = 6.78$ Hz).

^{13}C NMR (100 MHz, CDCl_3 , δ in ppm): 153.07, 139.65, 116.53, 110.79, 84.17, 75.89, 73.65, 69.26, 32.09, 32.06, 30.45, 29.88, 29.82, 29.78, 29.74, 29.55, 29.53, 29.50, 29.45, 26.23, 26.21, 22.84, 14.26.

FT-IR (cm^{-1}): 3315.10, 2959.40, 2923.29, 2854.86, 2106.45, 1574.74, 1501.01, 1468.80, 1421.62, 1380.56, 1333.95, 1234.64, 1116.84, 999.83, 832.38, 721.91, 680.20, 645.61, 596.63.

2.9 Synthesis of 1,2,3-tris(dodecyloxy)-5-ethynylbenzene (8b). The synthesis of the compound **8b** has been reported elsewhere.⁷



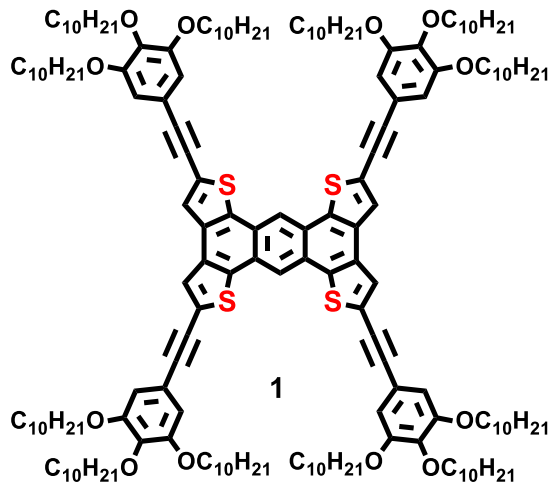
In a Schenk flask, addition of *n*-BuLi (1.6M in hexane) (7.98 mmol, 5.0 ml) to a solution of **7b** (3.19 mmol, 2.60g) in dry THF was carried out at $-78\text{ }^\circ\text{C}$ in a slow manner. Then the reaction was stirred for 24 hours at room temperature. After checking the TLC, the reaction was stopped and quenched with saturated NH_4Cl solution. After extraction with DCM, the organic layer was dried and evaporated to dryness and further subjected to purification. The purification by column chromatography using hexane-ethyl acetate as an eluent leads to obtain the product in 60 % yield as a solid white product.

^1H NMR (400 MHz, CDCl_3 , δ in ppm): δ 6.69 (s, 2H), 3.97-3.93 (m, 6H), 2.99 (s, 1H) 1.81-1.73 (m, 6H), 1.45-1.42 (m, 6H), 1.30-1.26 (m, 48H), 0.90-0.86 (t, 9H, $J = 6.76$ Hz).

^{13}C NMR (100 MHz, CDCl_3 , δ in ppm): 153.08, 139.65, 116.54, 110.80, 84.18, 75.89, 73.66, 69.27, 32.09, 30.45, 29.89, 29.85, 29.82, 29.79, 29.74, 29.53, 29.45, 26.24, 26.22, 22.85, 14.27.

FT-IR (cm^{-1}): 3314.22, 2959.40, 2924.07, 2853.85, 2110.90, 1575.33, 1500.33, 1467.40, 1420.66, 1380.04, 1333.94, 1234.89, 1117.36, 999.81, 831.91, 721.59, 645.55, 596.39.

2.10 Synthesis of tetrathienoanthracene derivative (1).



In an oven-dried double neck RBF, dry DMF (15 ml) and triethylamine (30 ml) was taken in 1:2 ratio. The solvent mixture was purged out vigorously with nitrogen for 30 minutes. Compound **5** (107 mg, 0.15 mmol) was then added and again purged it for 5 minutes. After that, addition of Pd(PPh₃)₄ (13.77 mg, 0.012 mmol) followed by CuI (2.8 mg, 0.015 mmol) was done and the reaction mixture was kept for stirring for further 10 minutes under N₂ atmosphere. Finally, addition of alkyne **8a** (680 mg, 1.19 mmol) was done and then stirred the reaction 110 °C for 3 days. The reaction was quenched with dilute HCl under cold condition and then extraction with ether was performed. The organic layer separation followed by evaporated to dryness and purification by using alumina-gel column chromatography enable to yield the orange-brown colored product in 36 % yield.

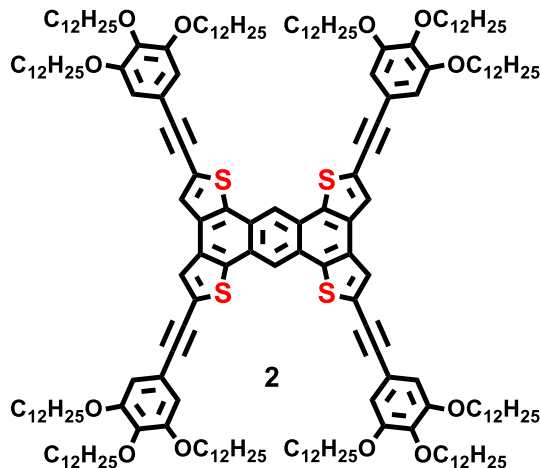
¹H NMR (400 MHz, CDCl₃, δ in ppm): δ 8.63 (s, 2H), 7.75 (s, 4H), 6.80 (s, 8H), 4.03-4.00 (m, 24H), 1.87-1.73 (m, 24H), 1.48-1.46 (m, 24H), 1.30-1.25 (m, 144H), 0.89-0.87 (m, 36H).

¹³C NMR (100 MHz, CDCl₃, δ in ppm): 153.23, 139.67, 135.92, 132.72, 127.48, 125.52, 123.74, 116.99, 110.10, 96.24, 81.82, 73.73, 69.31, 32.11, 30.58, 29.95, 29.87, 29.83, 29.67, 29.59, 29.56, 26.33, 22.87, 14.28.

FT-IR (cm⁻¹): 2955.50, 2923.51, 2853.61, 2202.20, 1738.00, 1574.14, 1510.25, 1502.00, 1468.06, 1422.20, 1376.50, 1354.59, 1308.00, 1236.76, 1119.02, 1018.80, 847.62, 824.06, 721.76.

MALDI-MS (m/z): M⁺ 2677.9734 (calculated for C₁₇₄H₂₆₆O₁₂S₄ = M⁺ 2677.9199).

2.11 Synthesis of tetrathienoanthracene derivative (2).



In an oven-dried double neck RBF, dry DMF (20 ml) and triethylamine (40 ml) was taken in 1:2 ratio. The solvent mixture was purged out vigorously with nitrogen for 30 minutes. Then compound **5** (183 mg, 0.255 mmol) was added and again purged it for 5 minutes. After that addition of Pd(PPh₃)₄ (23.55 mg, 0.020 mmol) followed by CuI (4.85 mg, 0.025 mmol) was done and the reaction mixture was kept for stirring for further 10 minutes under N₂ atmosphere. Finally addition of alkyne **8b** (1.33 g, 2.04 mmol) was done and then stirred the reaction 110 °C for 3 days. The reaction was quenched with dilute HCl under cold condition and then extraction with ether was performed. The organic layer separation followed by evaporated to dryness and purification by using alumina-gel column chromatography enable to yield the orange-brown colored product in 32 % yield.

¹H NMR (400 MHz, CDCl₃, δ in ppm): δ 8.62 (s, 2H), 7.75 (s, 4H), 6.80 (s, 8H), 4.03-4.00 (m, 24H), 1.87-1.73 (m, 24H), 1.50-1.41 (m, 24H), 1.30-1.25 (m, 192H), 0.89-0.86 (t, 36H, *J* = 5.80 Hz).

¹³C NMR (100 MHz, CDCl₃, δ in ppm): 153.27, 139.76, 136.00, 132.83, 127.96, 123.89, 119.18, 116.96, 110.20, 96.30, 81.73, 73.76, 69.35, 37.26, 32.91, 32.11, 30.56, 30.20, 29.95, 29.64, 29.56, 27.25, 26.32, 22.86, 19.89, 14.28.

FT-IR (cm⁻¹): 2955.50, 2923.29, 2853.12, 2206.00, 1738.00, 1574.26, 1505.10, 1466.97, 1422.20, 1376.50, 1352.06, 1236.48, 1117.98, 1030.30, 851.42, 823.83, 721.20.

MALDI-MS (*m/z*): M⁺ 3015.3357 (calculated for C₁₉₈H₃₁₄O₁₂S₄ = M⁺ 3015.2989).

3. NMR Spectral data:

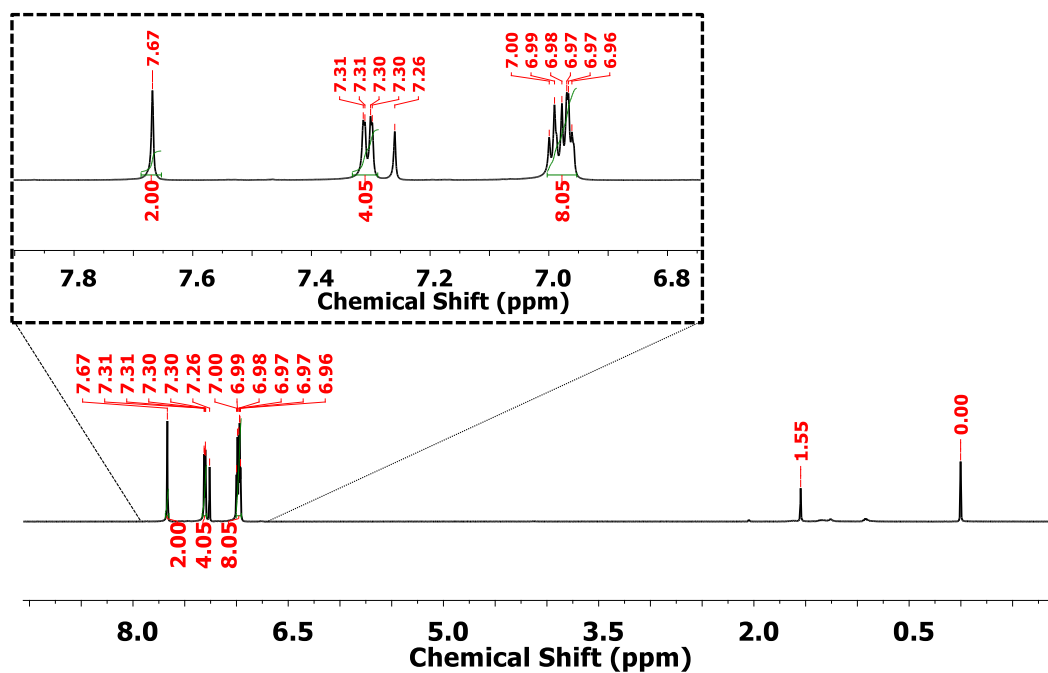


Figure S1. ¹H NMR spectrum of 3.

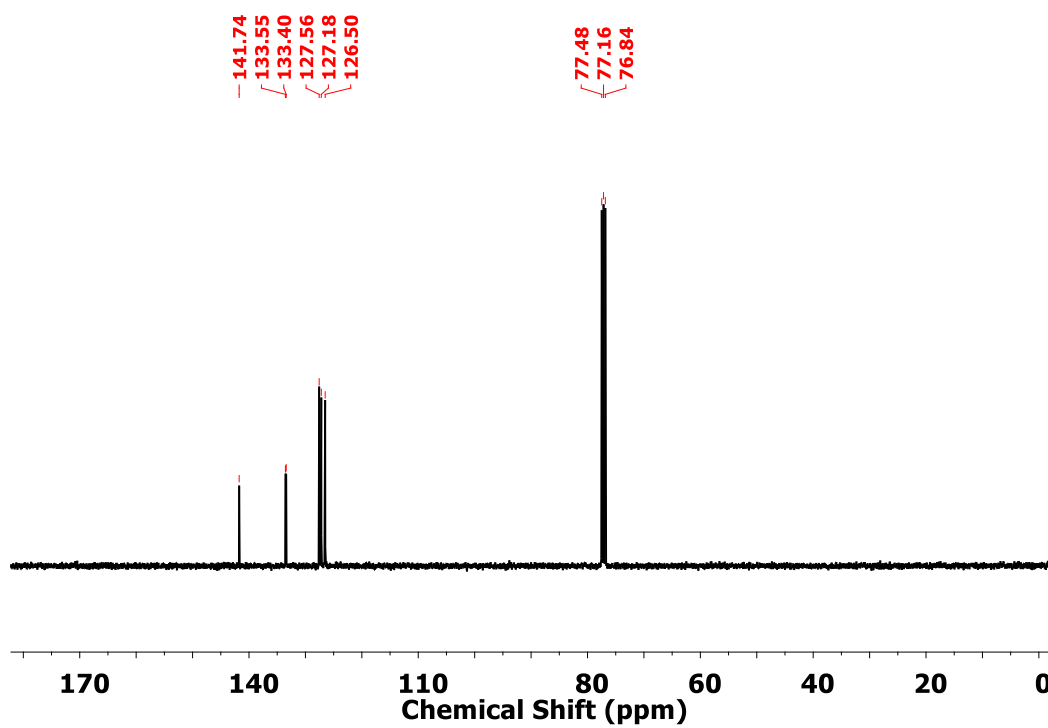


Figure S2. ¹³C NMR spectrum of 3.

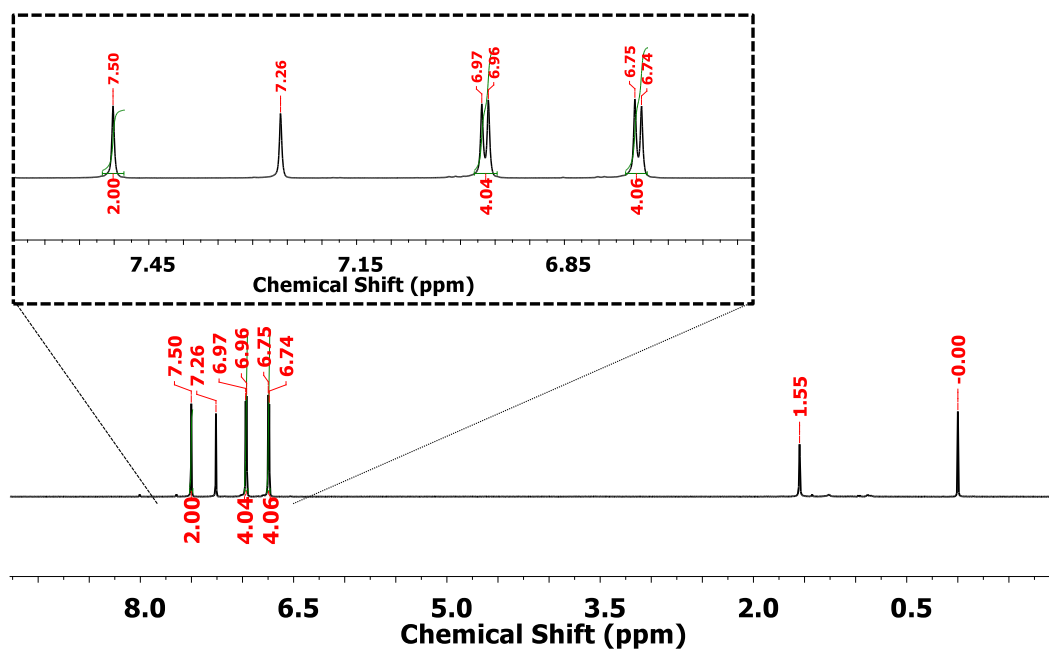


Figure S3. ^1H NMR spectrum of 4.

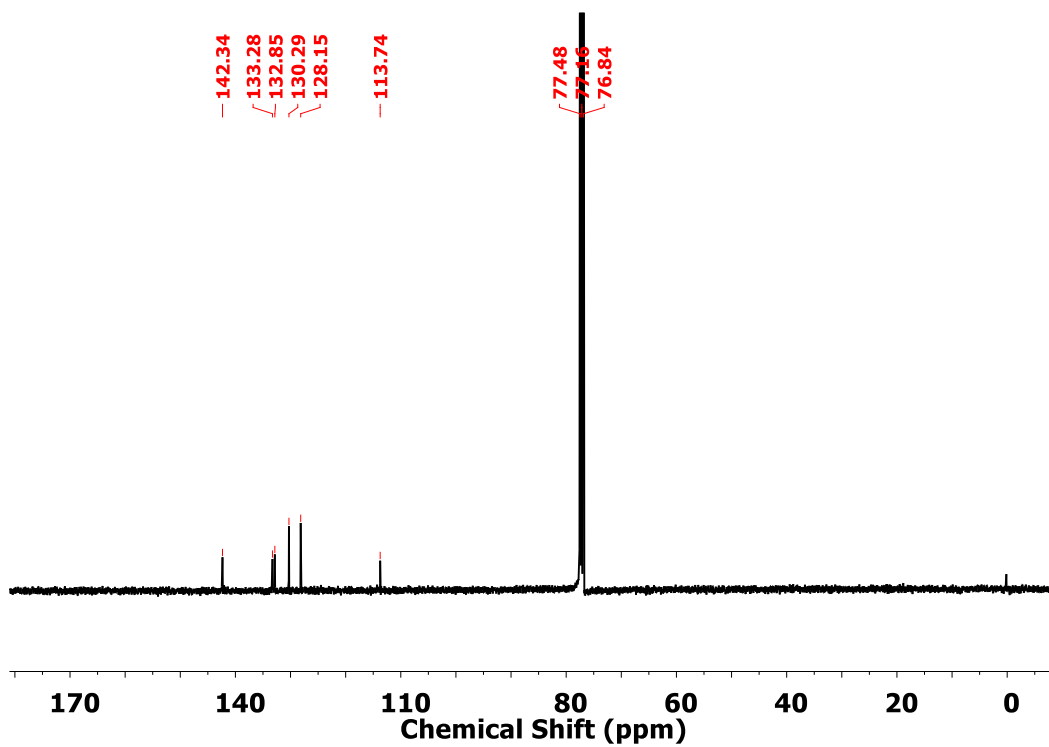


Figure S4. ^{13}C NMR spectrum of 4.

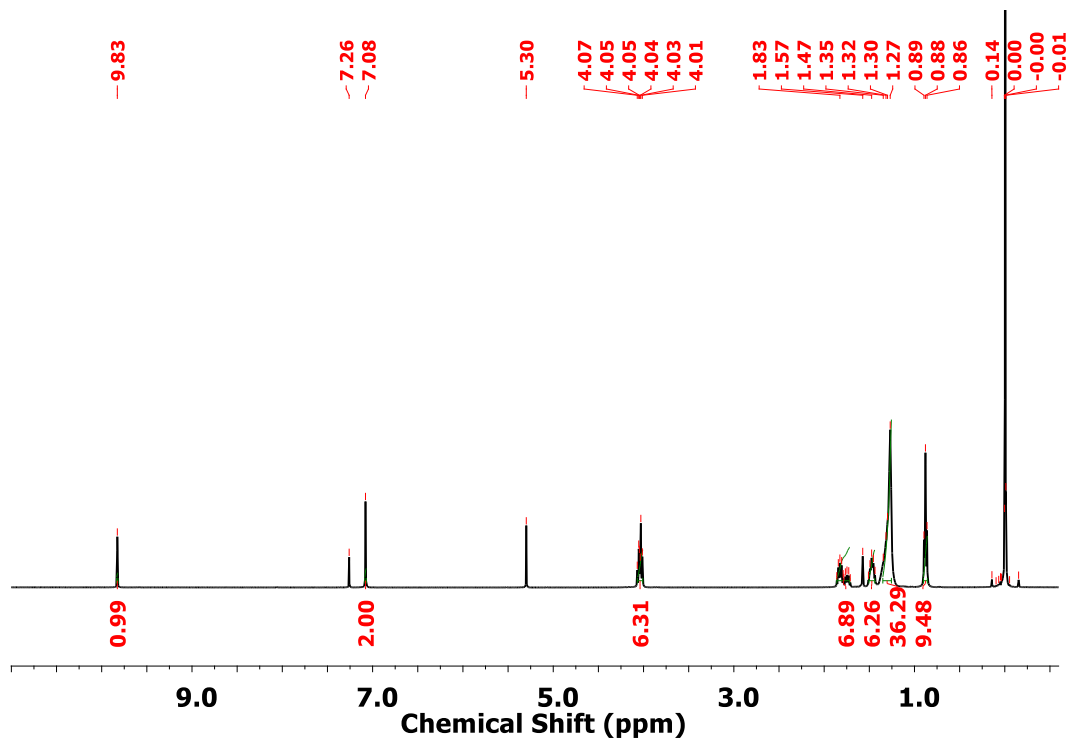


Figure S5. ^1H NMR spectrum of **6a**.

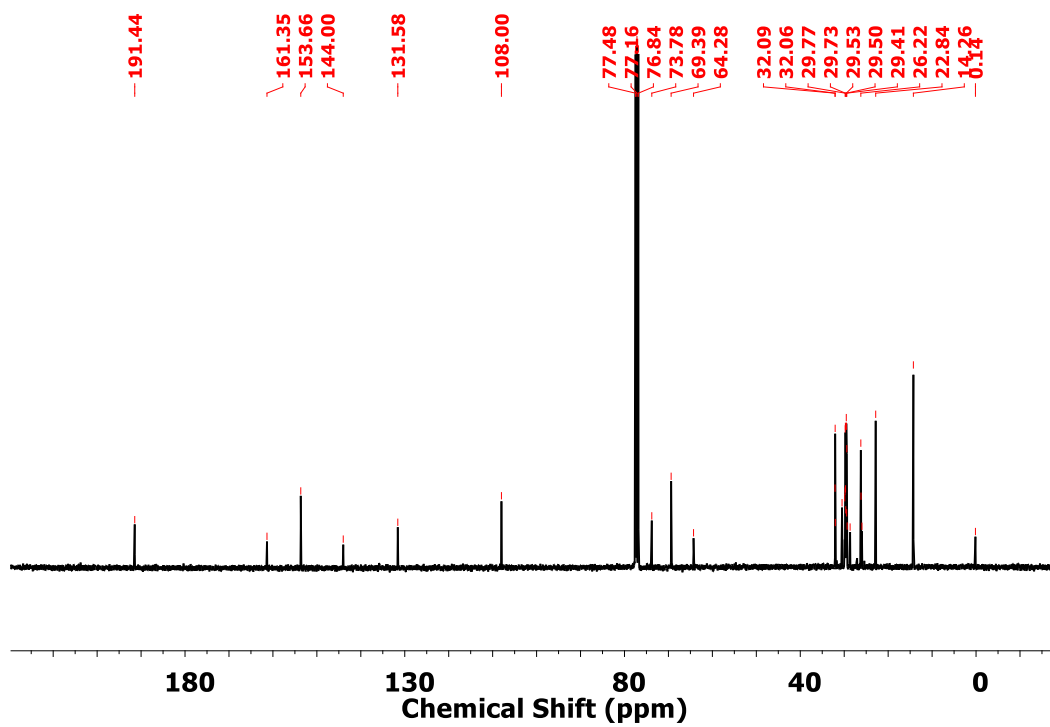


Figure S6. ^{13}C NMR spectrum of **6a**.

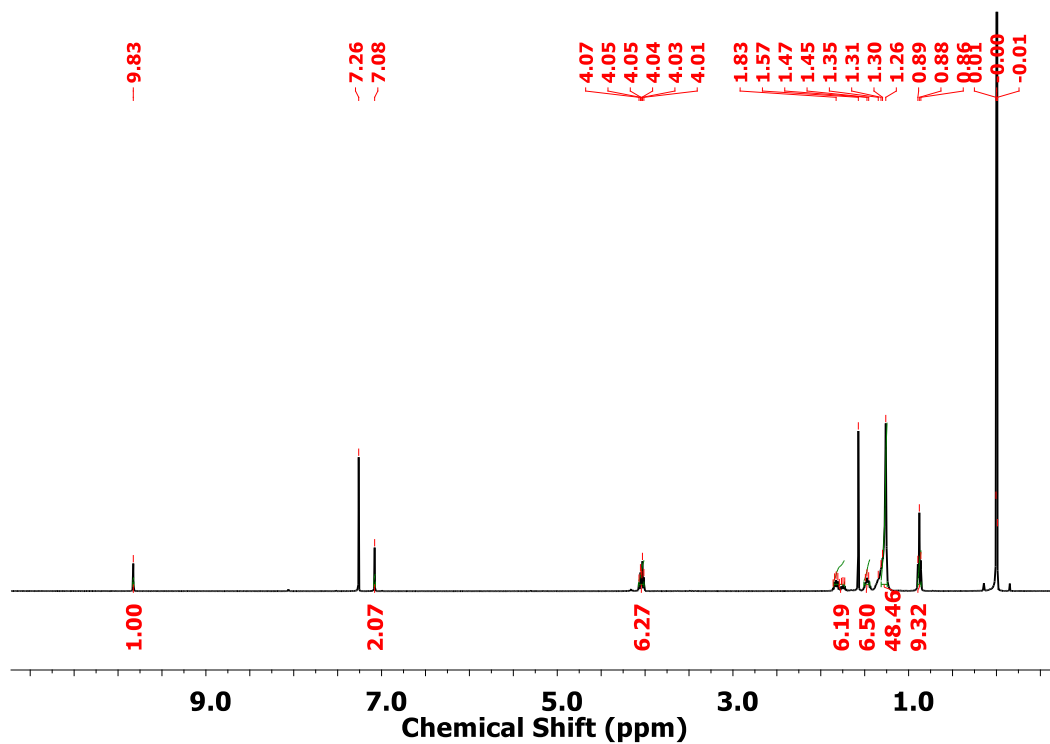


Figure S7. ^1H NMR spectrum of **6b**.

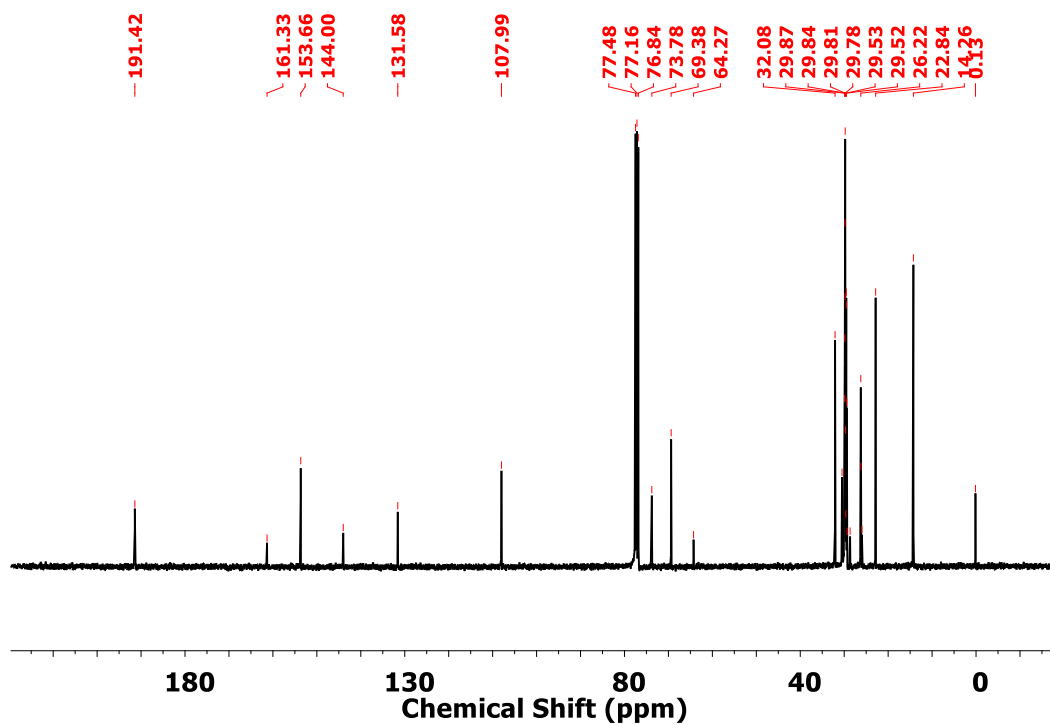


Figure S8. ^{13}C NMR spectrum of **6b**.

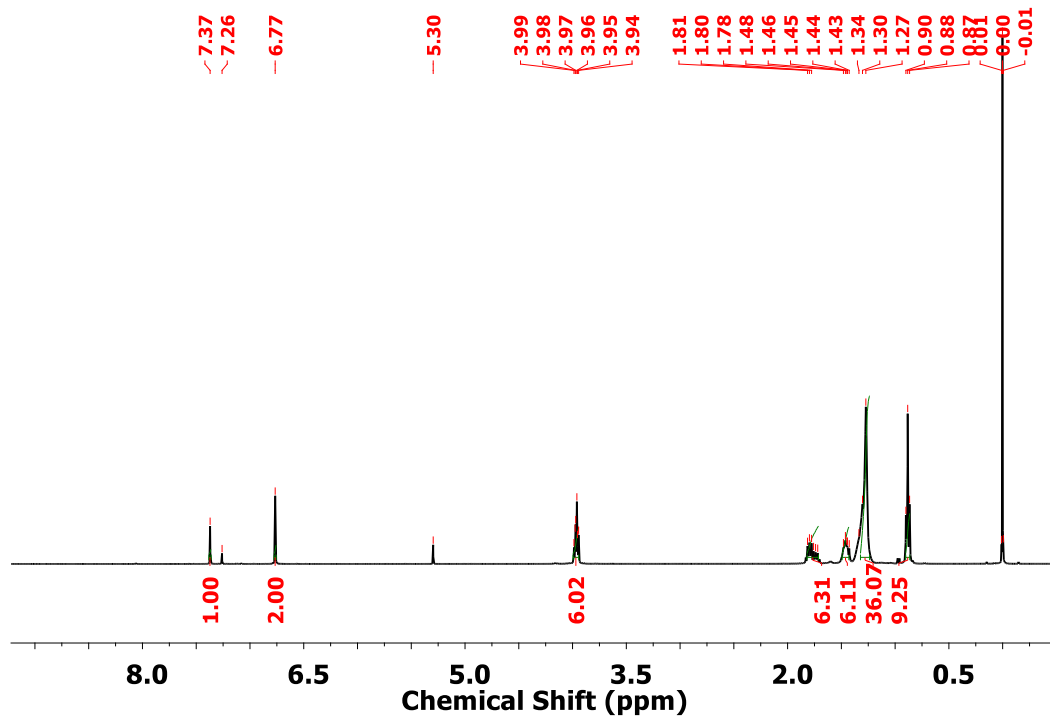


Figure S9. ¹H NMR spectrum of 7a.

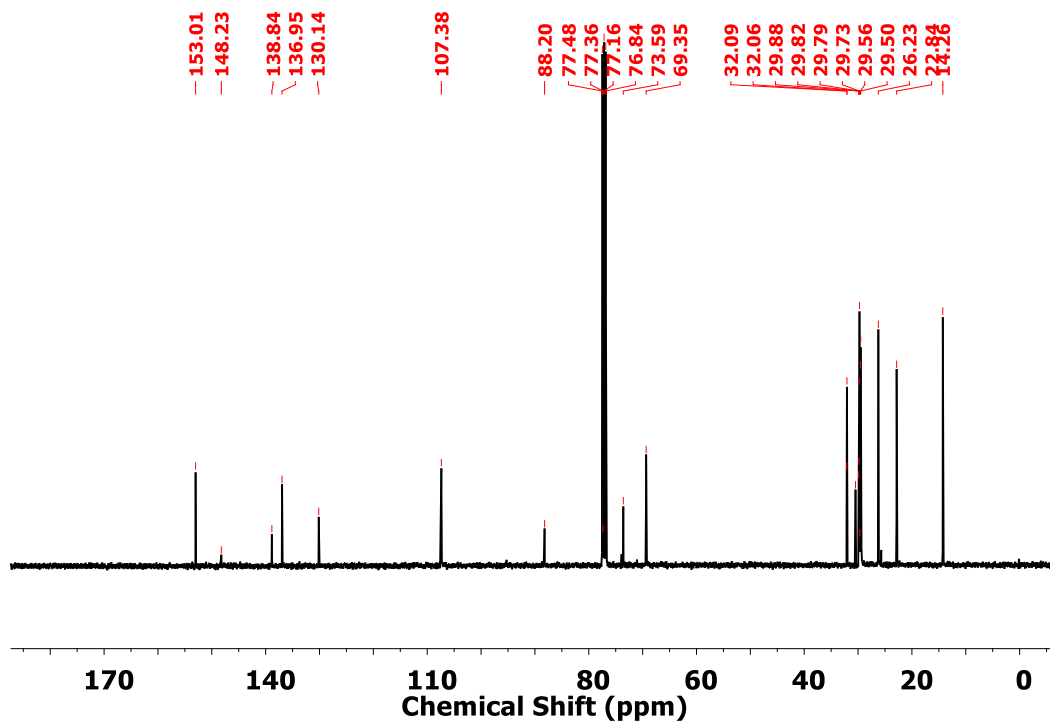


Figure S10. ¹³C NMR spectrum of 7a.

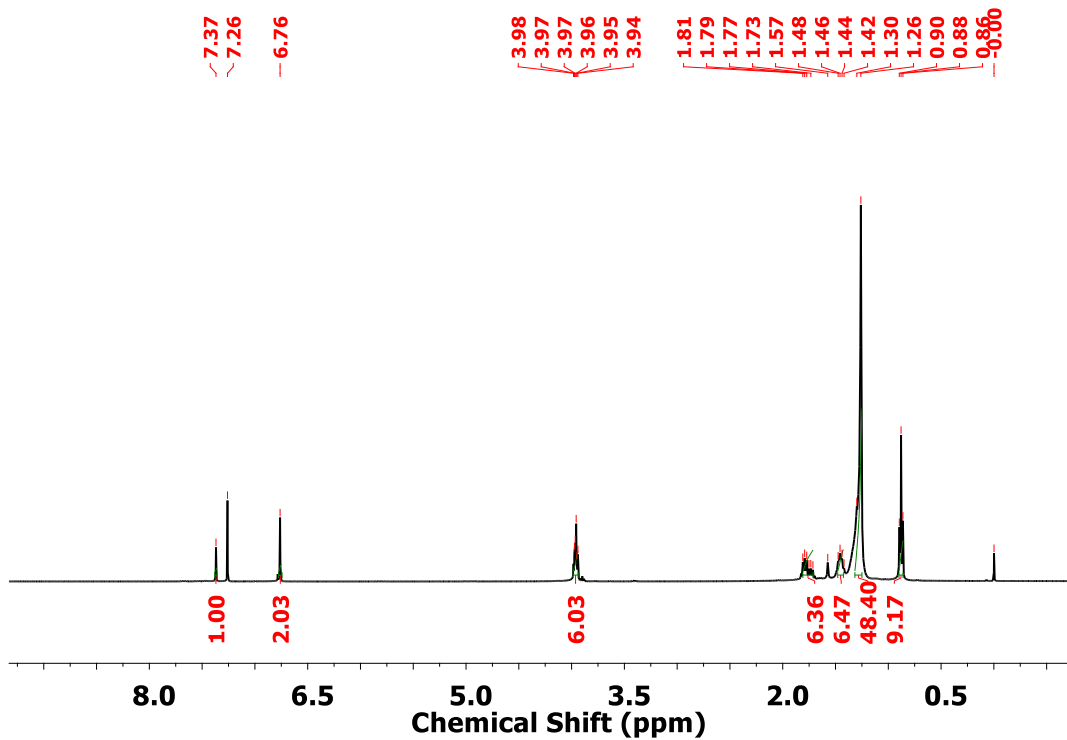


Figure S11. ¹H NMR spectrum of 7b.

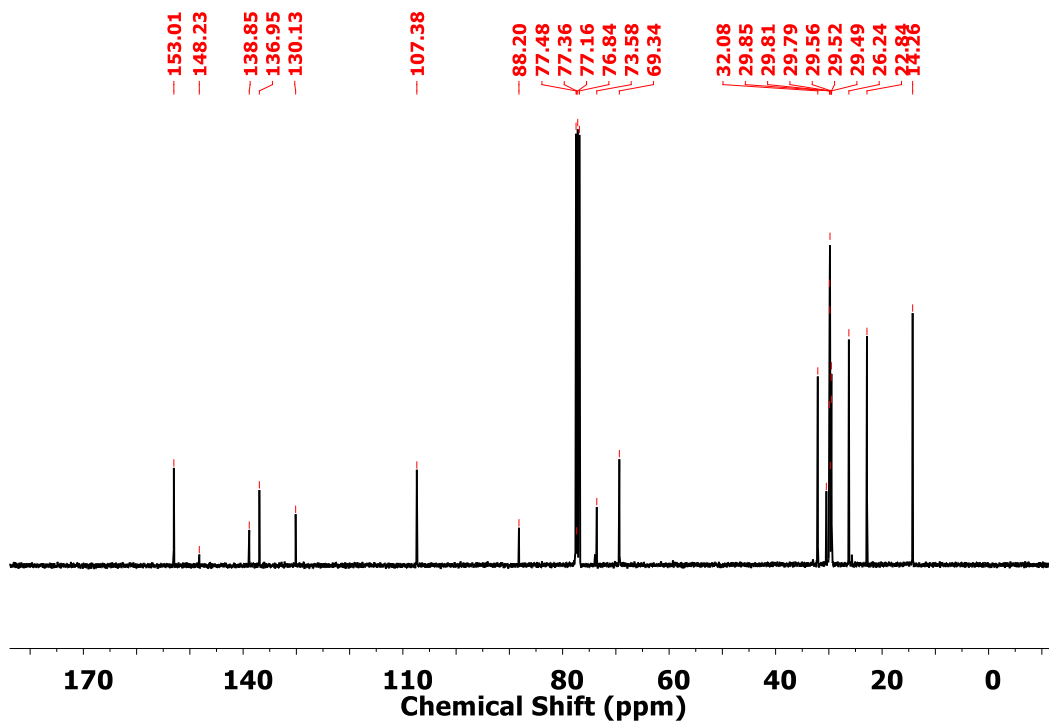


Figure S12. ¹³C NMR spectrum of 7b.

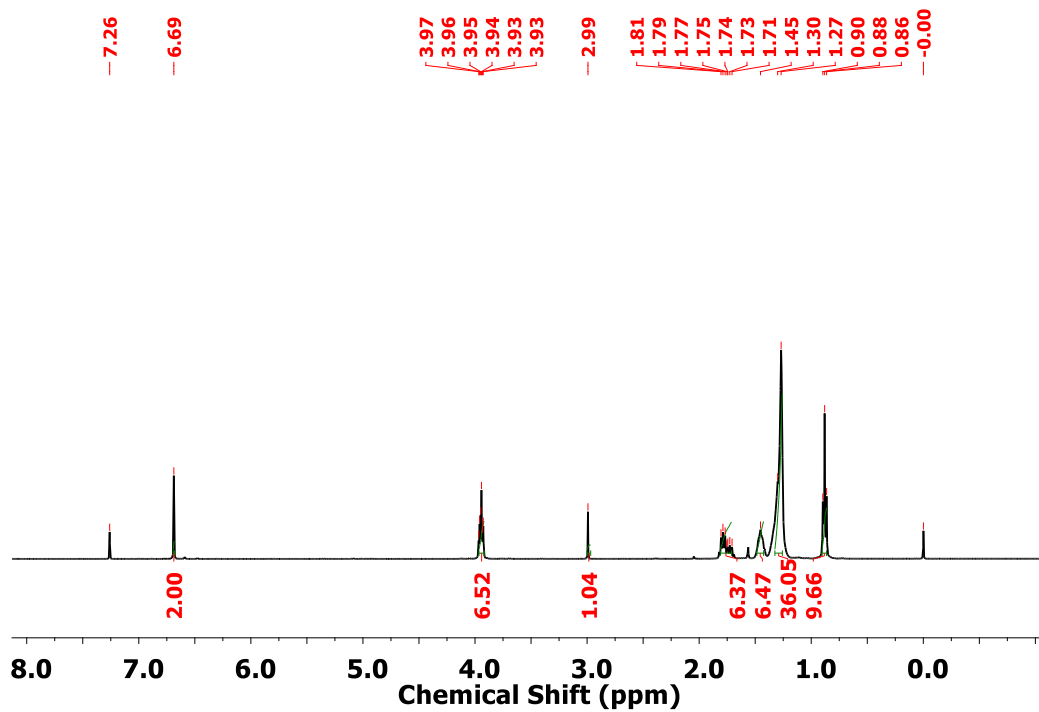


Figure S13. ¹H NMR spectrum of 8a.

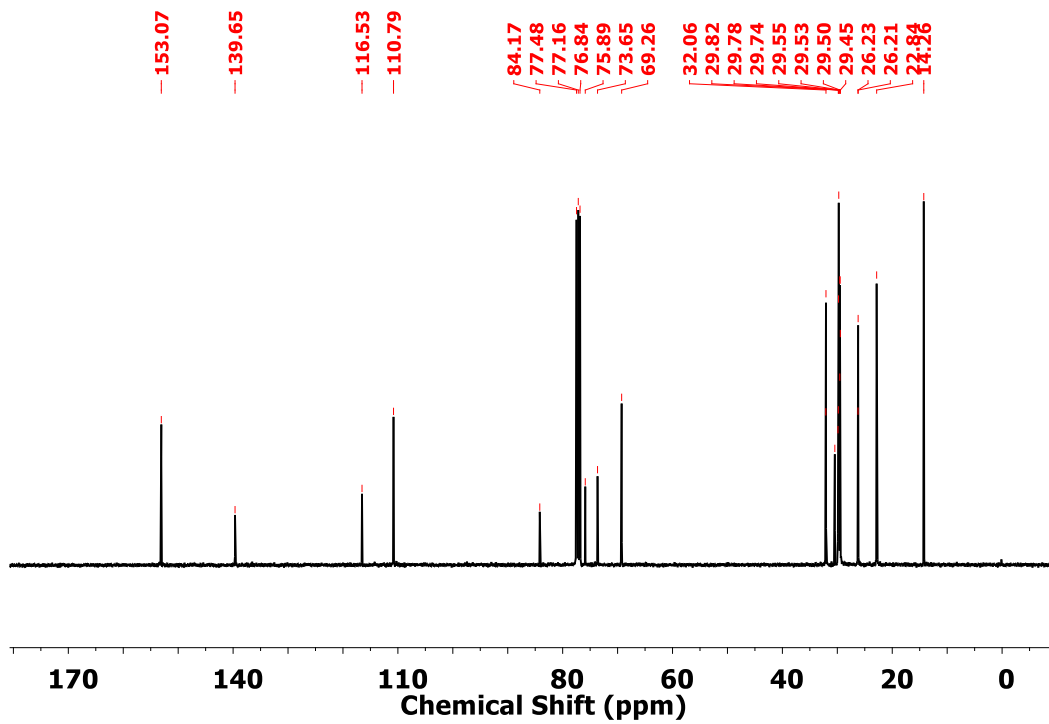


Figure S14. ¹³C NMR spectrum of 8a.

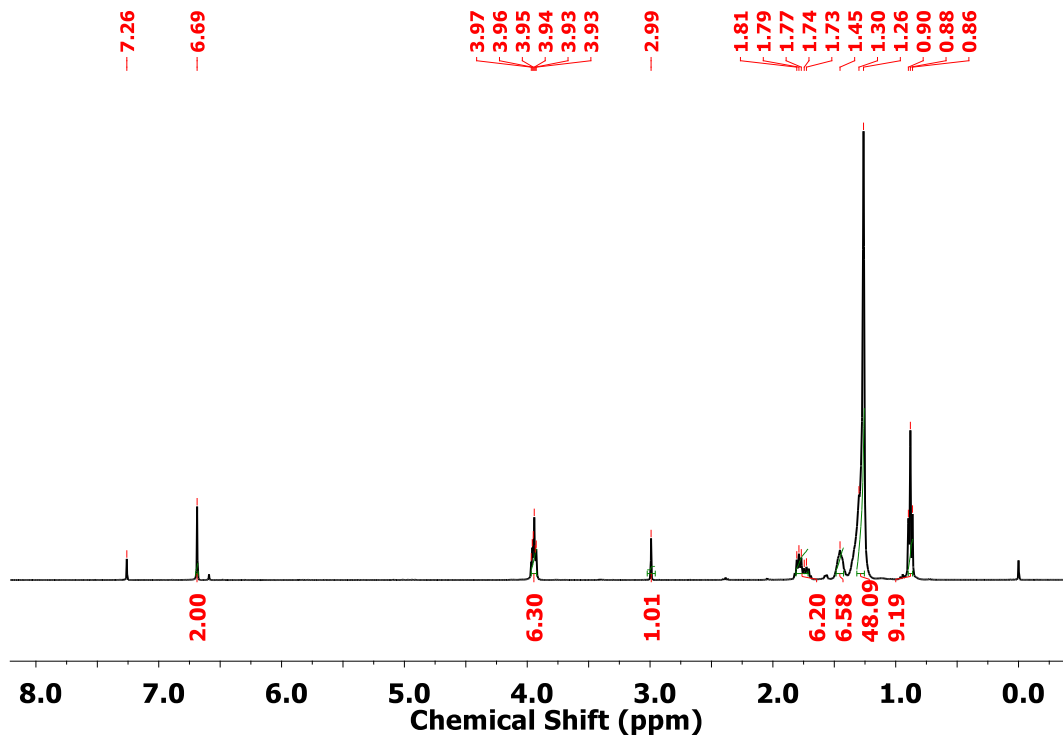


Figure S15. ¹H NMR spectrum of 8b.

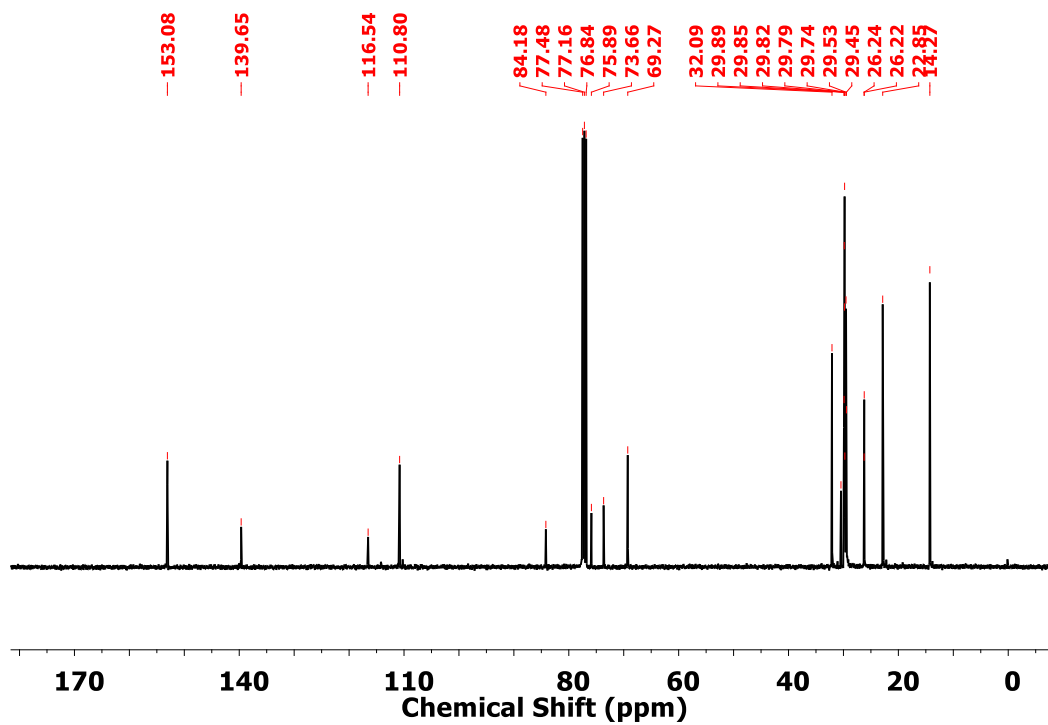


Figure S16. ¹³C NMR spectrum of 8b.

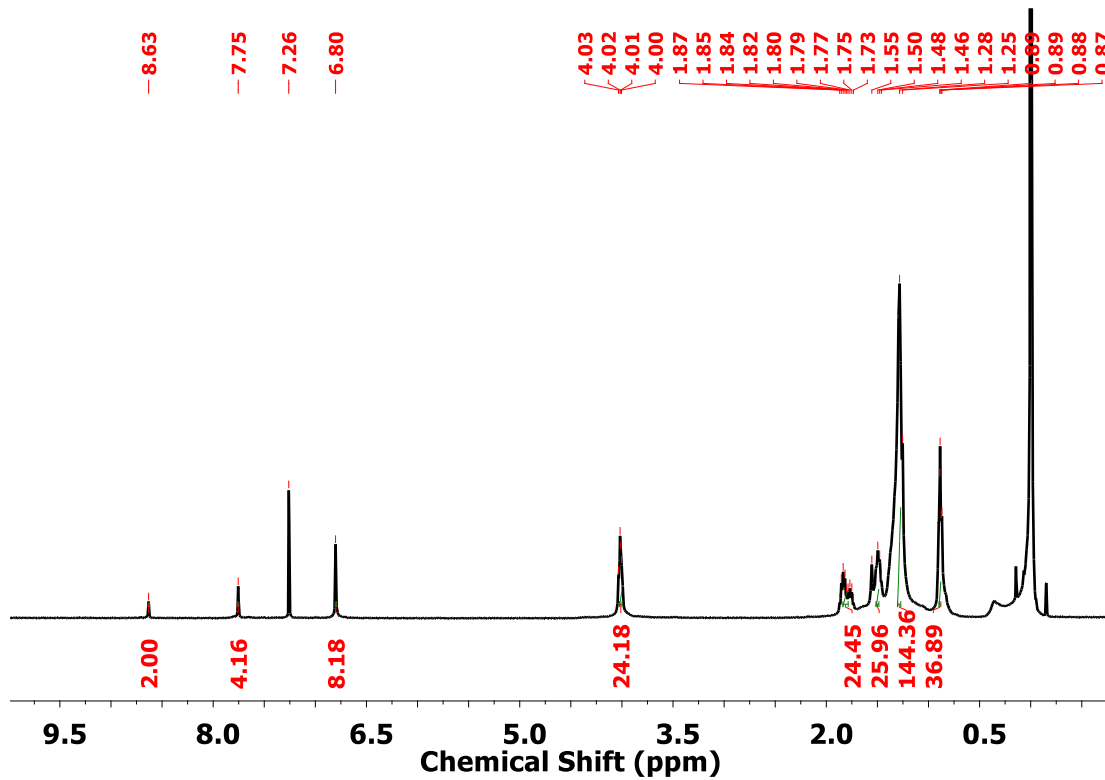


Figure S17. ^1H NMR spectrum of **1**.

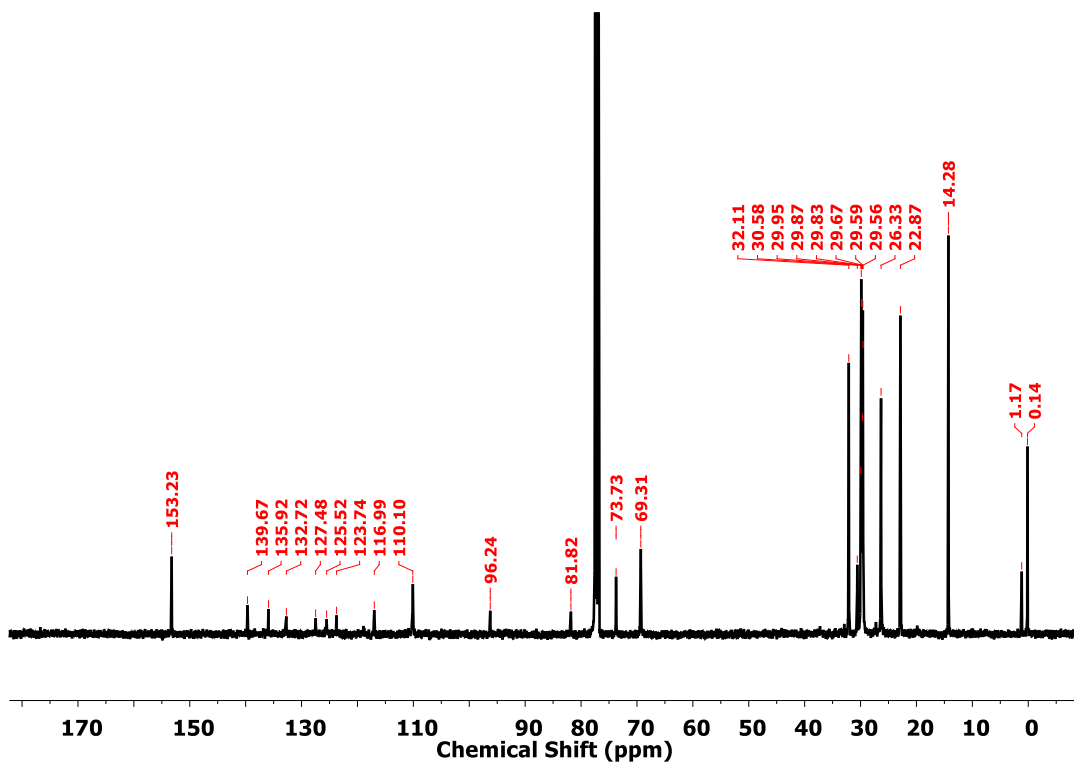


Figure S18. ^{13}C NMR spectrum of **1**.

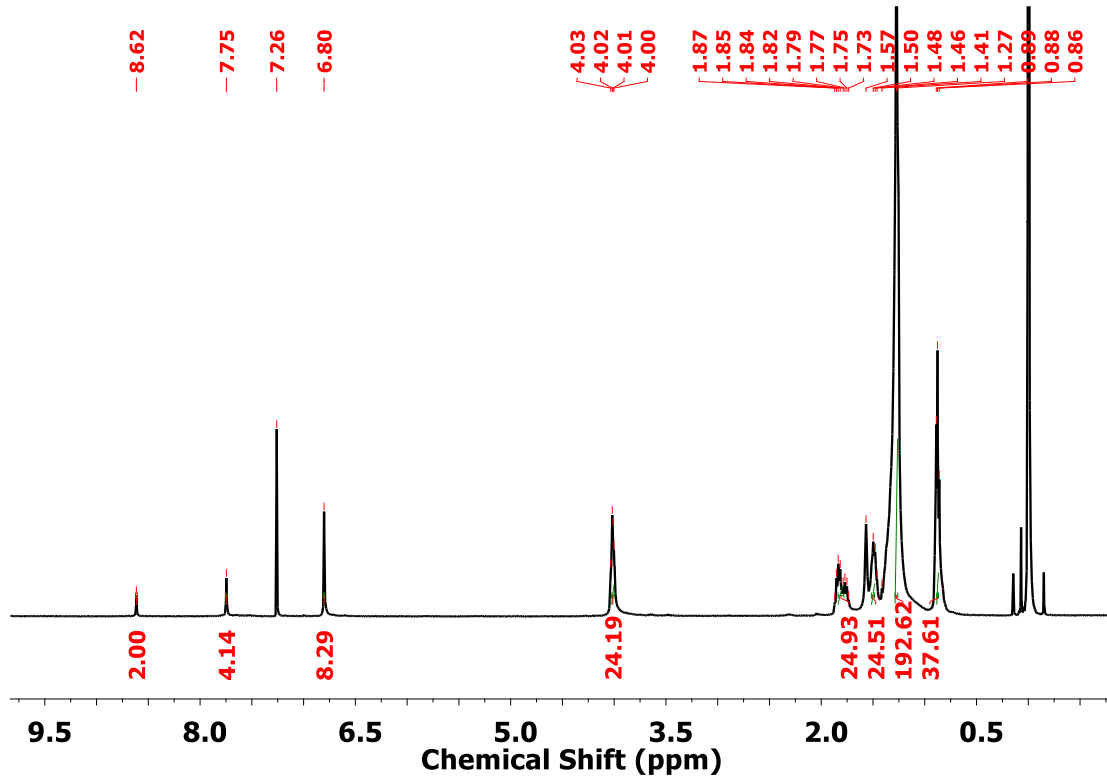


Figure S19. ^1H NMR spectrum of **2**.

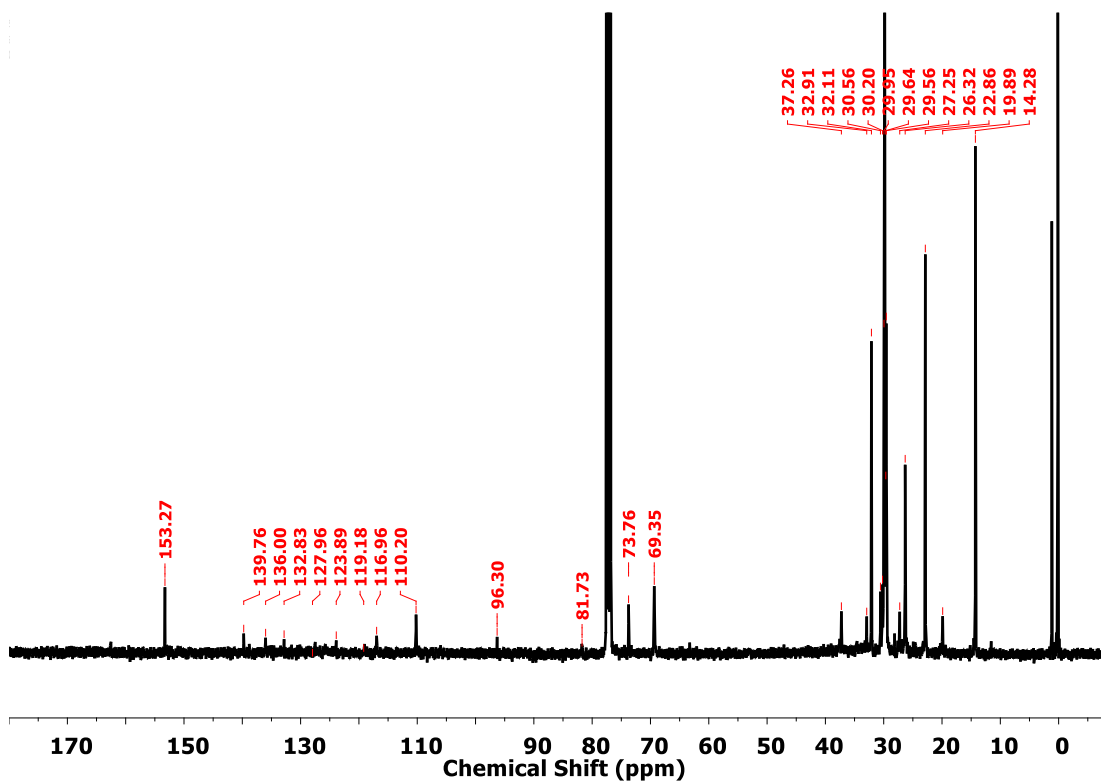


Figure S20. ^{13}C NMR spectrum of **2**.

4. Thermogravimetric analysis (TGA):

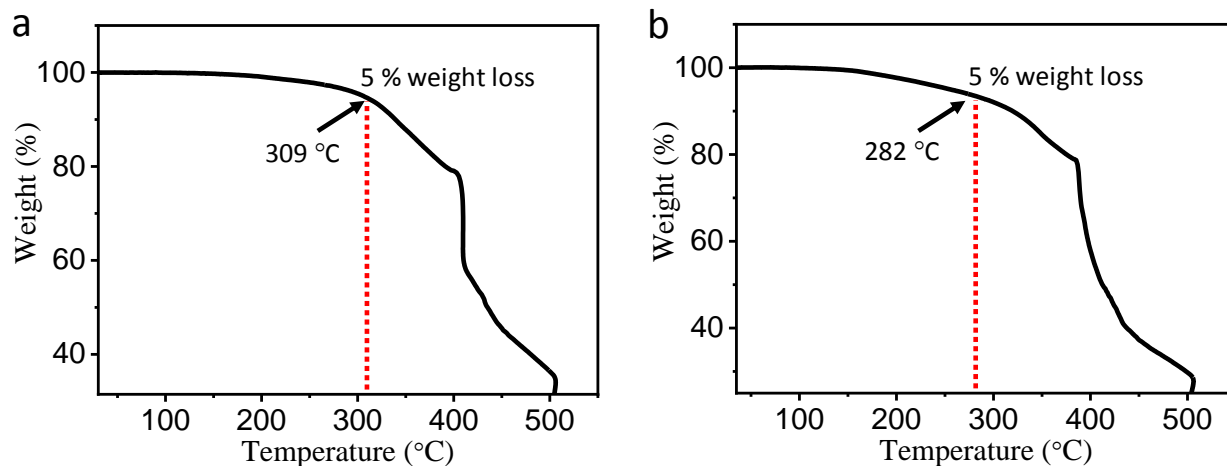


Figure S21. TGA curve of compound (a) **1** and (b) **2** recorded (rate 10 °C/min) under nitrogen atmosphere. Red dotted line indicates the decomposition temperature equivalent to ~5 % weight loss.

5. Polarised Optical Microscopy (POM) texture of TTA derivatives (Sample sandwiched between untreated/normal glass slides):

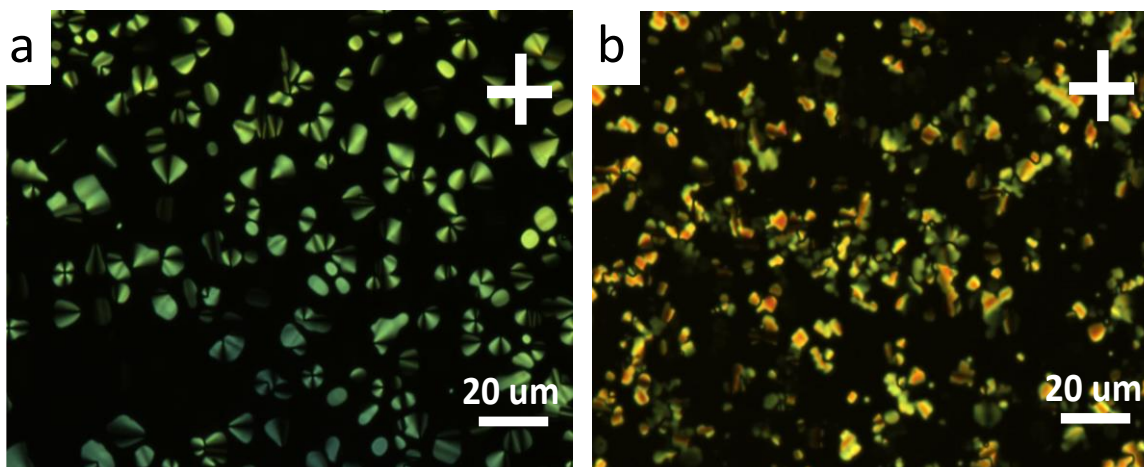


Figure S22. Microscopic texture of compound **2** sandwiched between normal glass slides: (a) at 117.1 °C and (b) at 49.9 °C recorded with the rate of 10 °C/min under crossed polarizer (magnification $\times 500$).

6. Differential Scanning Calorimetry (DSC) thermogram:

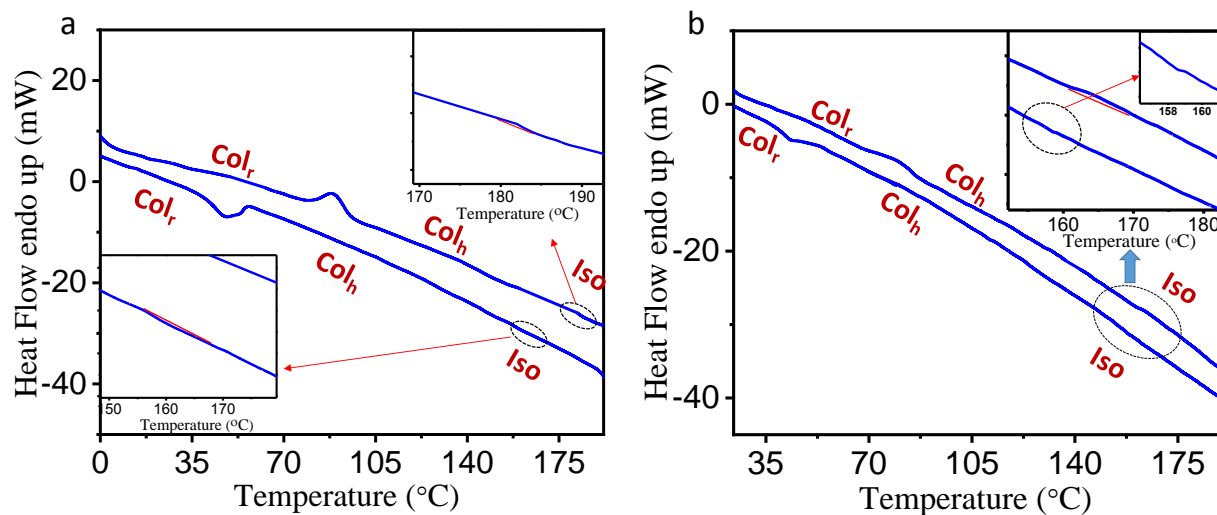


Figure S23. DSC thermogram of compound (a) **1** and (b) **2** recorded with the scan rate of 10 °C/min.

7. X-Ray diffraction data:

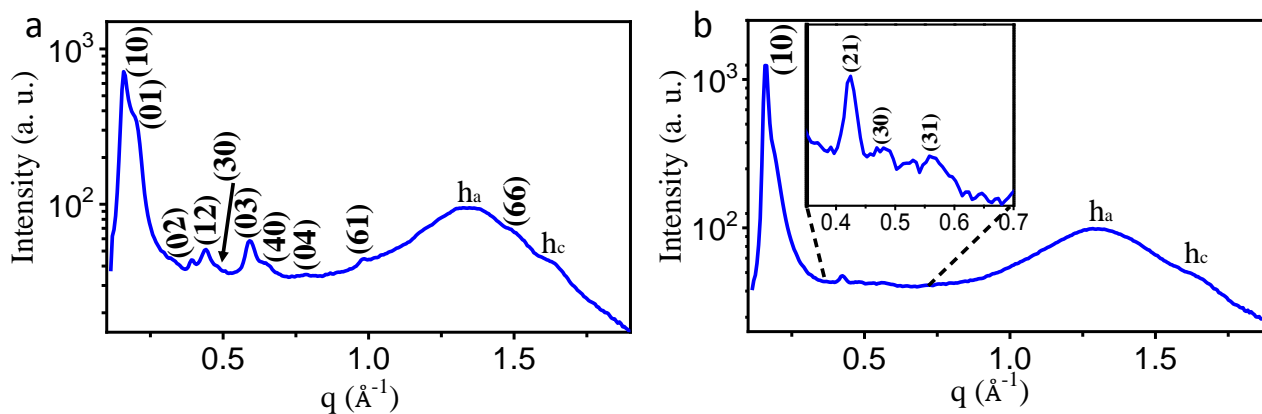


Figure S24. X-Ray diffraction pattern of **2** (a) at 30 °C in columnar rectangular (Col_r) phase and (b) at 90 °C in columnar hexagonal (Col_h) phase.

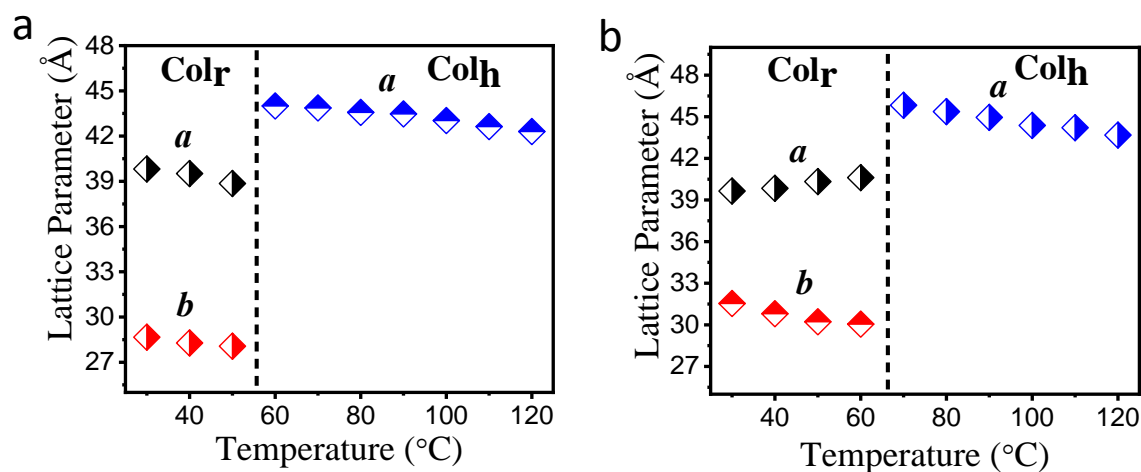


Figure S25. Variation of lattice parameter of compound (a) **1** and (b) **2** with temperature (on cooling). In the Col_r phase ‘a’ and ‘b’ represents the lattice parameter. In the Col_h phase ‘a’ shows the inter-columnar separation.

Table S1. Phase behavior, Miller Indices, lattice constants and *d*-spacing observed from the X-ray diffraction studies for compound **1**.

TM ^a	Mesophase	Lattice constants (Å)	<i>d</i> _{obs} ^b (Å)	<i>d</i> _{cal} ^c (Å)	MI ^a (<i>hk</i>)	RI (Φ)(M) ^a
1	Col _r at 30 °C	<i>a</i> = 39.81	39.82	39.81	10	100.00(0)(2)
		<i>b</i> = 28.66	28.66	28.66	01	30.07(0)(2)
			20.08	19.90	20	6.49(π)(2)
			13.60	13.48	12	7.42(0)(4)
			9.80	9.95	40	6.36(π)(2)
			8.88	8.61	23	5.30(0)(4)
			5.93	6.02	62	
			4.77	4.78	06	
			4.09	4.09	84	
	3.74		h_c			
	Col _h at 95 °C	<i>a</i> = 43.44	37.62	37.62	10	100.00(0)(6)
		14.21	14.22	21	3.73(π)(12)	
		12.54	12.54	30	3.29(0)(6)	
		8.22	8.21	41	3.37(0)(12)	
4.87			h_a			
3.85		h_c				

^b*d*_{obs}: experimental *d*-spacing; ^c*d*_{cal}: calculated *d*-spacing by using the relation for Col_r: $\frac{1}{d_{cal}^2} = \left[\frac{h^2}{a^2} + \frac{k^2}{b^2} \right]$; Col_h: $\frac{1}{d_{cal}^2} = \left[\frac{4}{3} \left(\frac{h^2 + hk + k^2}{a^2} \right) + \frac{l^2}{c^2} \right]$; *h*, *k*, *l*: Miller indices of observed reflections; *a*, *b* & *c*: unit cell parameters, h_a: alkyl

chain-chain correlation; h_c : core-core correlation. ^aAbbreviations: TM- Target Material; MI- Miller Indices; RI (Φ)(M)- Relative Intensity (Phase value)(Multiplicity).

Table S2. Phase behavior, Miller Indices, lattice constants and d -spacing observed from the X-ray diffraction studies for compound **2**.

TM ^a	Mesophase	Lattice constants (Å)	d_{obs}^b (Å)	d_{cal}^c (Å)	MI ^a (hk)	RI (Φ)(M) ^a
2	Col _r at 30 °C	$a = 39.64$	39.64	39.64	10	100.00 (0)(2)
		$b = 31.54$	31.54	31.54	01	51.26(0)(2)
			15.85	15.77	02	6.02(0)(2)
			14.41	14.65	12	7.14(π)(4)
			13.09	13.21	30	2.80(0)(2)
			10.63	10.51	03	8.12(0)(2)
			9.72	9.91	40	
			8.00	7.89	04	
			6.41	6.47	61	
			4.65		h_a	
			4.19	4.11	66	
		3.82		h_c		
	Col _h at 90 °C	$a = 45.44$	39.35	39.35	10	100.00(0)(6)
			14.80	14.87	21	3.80(π)(12)
			13.13	13.12	30	3.47(0)(6)
			10.94	10.91	31	3.39(0)(12)
			4.87		h_a	
			3.81		h_c	

^b d_{obs} : experimental d -spacing; ^c d_{cal} : calculated d -spacing by using the relation for Col_r: $\frac{1}{d_{cal}^2} = \left[\frac{h^2}{a^2} + \frac{k^2}{b^2} \right]$; Col_h: $\frac{1}{d_{cal}^2} = \left[\frac{4}{3} \left(\frac{h^2+hk+k^2}{a^2} \right) + \frac{l^2}{c^2} \right]$; h, k, l : Miller indices of observed reflections; a, b & c : unit cell parameters, h_a : alkyl chain-chain correlation; h_c : core-core correlation. ^aAbbreviations: TM- Target Material; MI- Miller Indices; RI (Φ)(M)- Relative Intensity (Phase value)(Multiplicity).

Electron density Map: The procedure to reconstruct the electron density maps (EDMs) are reproduced herein as per reported in the previous reports for the convenience to the readers.¹⁻⁴

“The electron density $\rho(x,y)$ of a liquid crystal is associated to its structure factor $F(hk)$ by inverse Fourier transformation:

$$\rho(x,y) = \sum_{h,k} F(hk) e^{2\pi i(hx+ky)}$$

where (hk) are the Miller Indices and x, y are fractional coordinates in the unit cell.

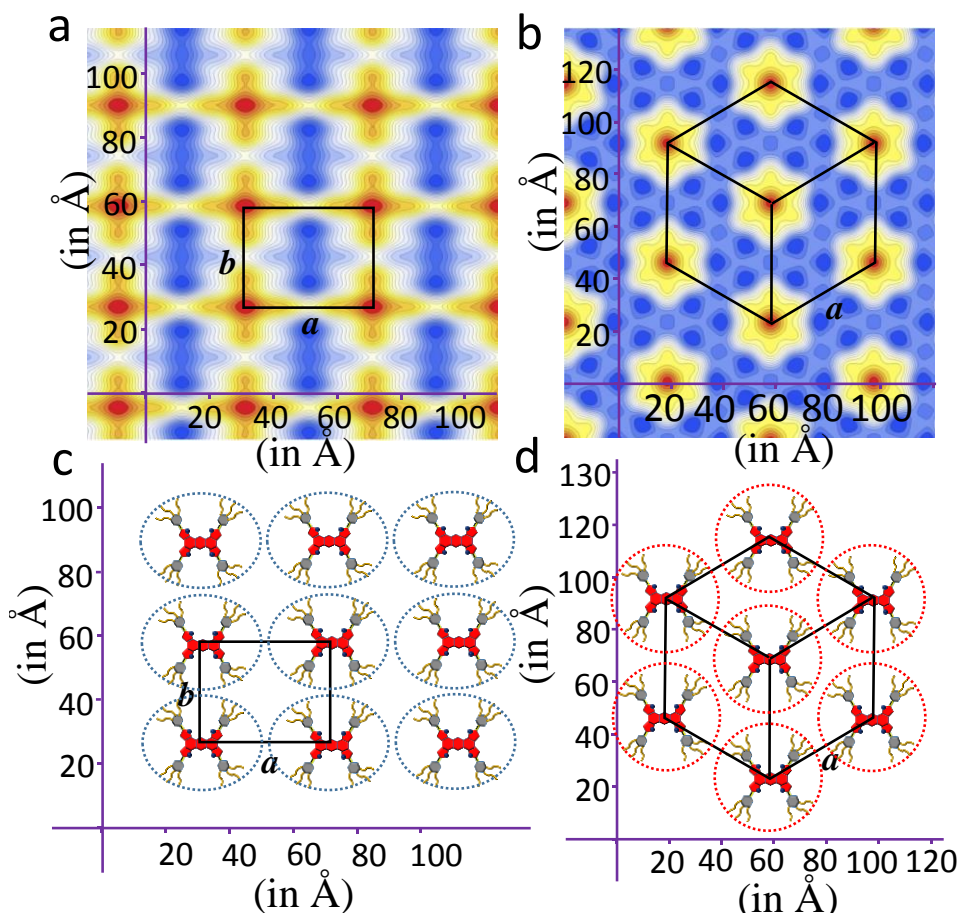


Figure S26. EDMs of compound **2** in (a) Col_r phase at temperature 30 °C and (b) Col_h phase at temperature 90 °C. Red color in the EDM correspond to high electron density region while lowest electron density areas are represented by deep blue color. Rectangle in Figure (a) draws the unit cell of Col_r phase with lattice parameter ‘ a ’ & ‘ b ’ and hexagon in Figure (b) displayed the conventional unit cell of Col_h phase with lattice parameter ‘ a ’. (c) & (d) exhibit the corresponding molecular arrangement in the Col_r and Col_h phase, respectively.

To estimate the electron density, the complex structure factor (hk) which is equal to the product of the phase $\Phi(hk)$ and the modulus $|hk|$ and proportional to the square root of the intensity $I(hk)$ of the observed reflection as given below:

$$F(hk) = |F(hk)|e^{i\Phi(hk)} = \sqrt{I(hk)}e^{i\Phi(hk)}$$

While the intensity $I(hk)$ can be simply obtained from the X-ray diffraction experiment, the only information that cannot be obtained directly from experiment is the phase $\Phi(hk)$ for each diffraction peak. However, this problem becomes easily tractable when the structure under study is centro-symmetric, that if $\rho(x,y)=\rho(-x,-y)$, $F(hk)$ can only be real hence, $\phi(hk)$ can only be 0 or π . For noncentro-symmetric groups, the phase may take every value between 0 and 2π . Since the columnar phase observed in case of compounds **1** and **2** are centro-symmetric and have only limited number of diffraction peaks, it is possible to reconstruct electron density maps of all possible phase combinations. The “correct” map is subsequently chosen on the merit of the reconstructed maps and other physical and chemical knowledge of the system such as, chemical constituents and their sizes *etc.*”

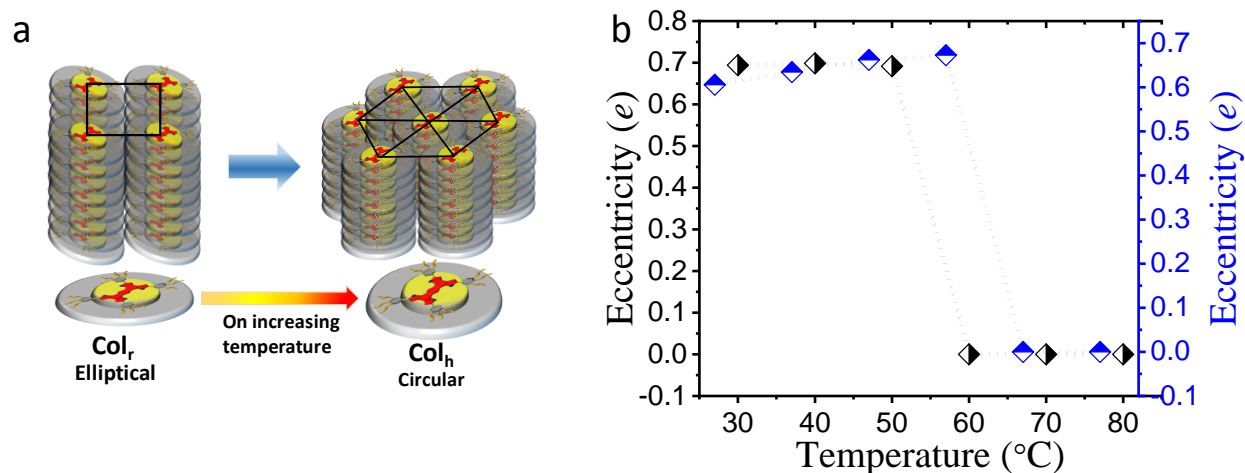


Figure S27. (a) Schematic showing the switching of Col_r to Col_h due to shape change of the molecule. (b) Variation of eccentricity (e) of compound with temperature on cooling. Black and Blue diamond represents the variation for compound **1** and **2**, respectively. Eccentricity is calculated by assuming the elliptical shape and circular shape of the compound in Col_r and Col_h phase, respectively.

8. Photophysical, Electrochemical and Theoretical studies:

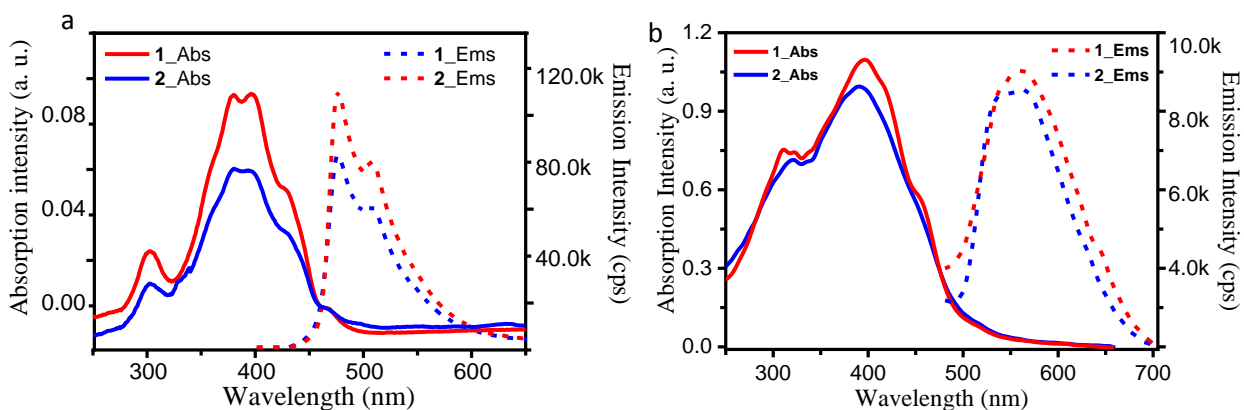


Figure S28. Absorption (Abs) and emission (Ems) spectra of compound **1** and **2** (a) in solution state (chloroform) and (b) in thin film state.

Table S3. Photophysical data of the TTA derivatives.

C	A_{solution}^a Peaks (nm)	E_{solution}^{a,c} Peaks (nm)	A_{solid} Peaks (nm)	E_{solid}^{c*} Peaks (nm)
1	303, 380, 396, ^b 423, 469	476, 507, 545*	323, 398, ^b 455, 515	537, 560, 645
2	303, 380, 395, ^b 428, 467	475, 506, 546*	321, 390, ^b 454, 515	540, 563, 634

^ain micromolar chloroform solution. ^bExcitation wavelength, λ_{exc} . ^cobtained after exciting at respective λ_{exc} . *Peaks can be visualised after zooming the respective region. Abbreviation: C: Compound, A_{solution}: Solution state absorbance, E_{solution}: Solution state emission. A_{solid}: Thin-film absorbance, E_{solid}: Thin-film emission.

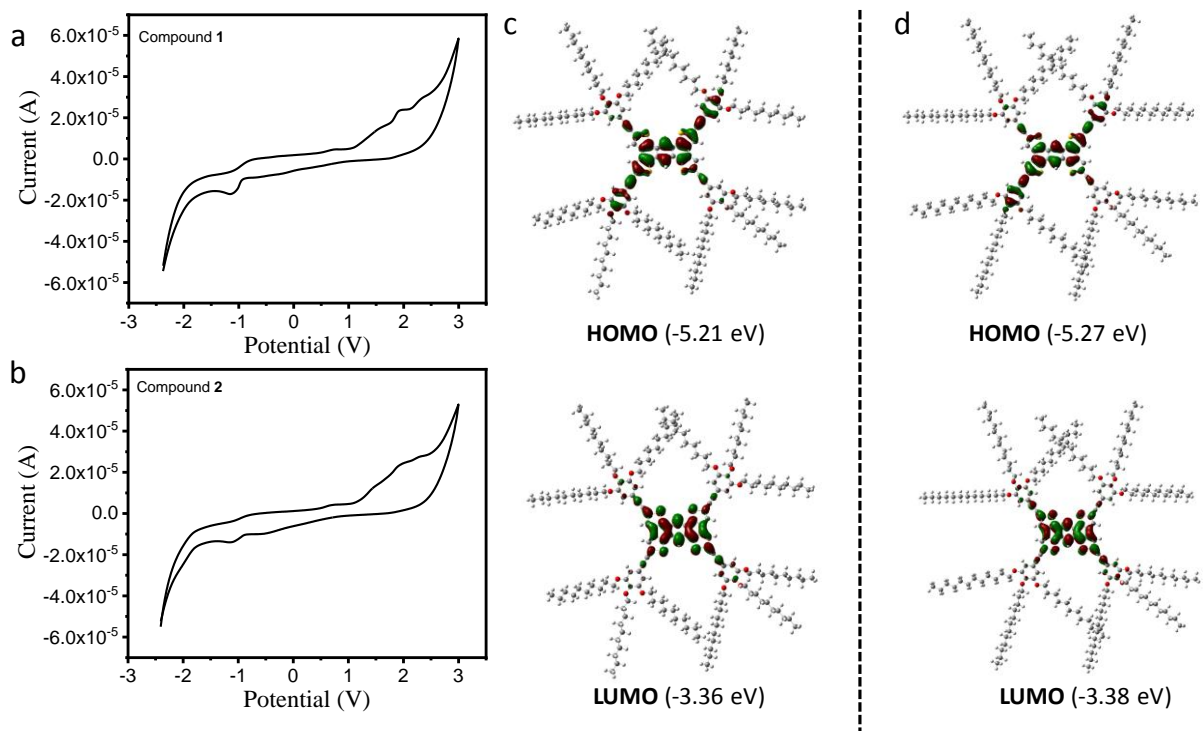


Figure S29. Cyclic Voltammograms of compound (a) **1** and (b) **2** in HPLC dichloromethane solution of tetrabutylammonium hexafluorophosphate (0.1 M) performed at a scanning rate 50 mVs⁻¹. Frontier molecular orbitals of compound (c) **1** and (d) **2** obtained by using B3LYP/6-31G (d,p) basis set.⁸

Table S4. Electrochemical properties of TTA derivatives.^a

Compound	E _{red} (V) ^b	E _{oxd} (V) ^c	E _{LUMO} (eV) ^d	E _{HOMO} (eV) ^e	ΔE _{g,CV} (eV) ^f	ΔE _{g,opt} (eV) ^g
1	-0.89	+1.02	-3.36	-5.21	1.85	2.04
2	-0.86	+0.96	-3.38	-5.27	1.89	2.06

^aExperimental conditions: reference electrode-Ag/AgNO₃ electrode, counter electrode-platinum wire electrode, working electrode-glassy carbon electrode, supporting electrolyte-tetrabutylammonium perchlorate (0.1 M). ^bReduction onset potential. ^cOxidation onset potential. Estimated from the formula: ^dE_{LUMO} = -(4.8 - E_{1/2,Fc,Fc⁺} + E_{red,onset}) eV. ^eE_{HOMO} = -(4.8 - E_{1/2,Fc,Fc⁺} + E_{oxd,onset}) eV. ^fElectrochemical band gap: ΔE_{g,CV} = E_{LUMO} - E_{HOMO}. ^gOptical band gap estimated from red absorption edge.

9. Mobility Studies by Space Charge Limited Current (SCLC):

9.1 Sample Fabrication: The similar procedure has been adopted to fabricate the samples for SCLC measurement as that of our previous paper.⁹

“For SCLC measurements, cells were prepared using FTO (Xinyan Technologies, Taiwan, 7 Ω/cm^2) and Gold (Au) Electrodes. FTO substrates were patterned using zinc powder and 2M hydrochloric acid (Sigma Aldrich) solution. Firstly, the FTO substrate was masked using Kapton tape of required dimension (1 to 1.5 mm), then the unmasked area was covered using Zinc Powder. 2M HCl solution was then added drop wise to cover the entire substrate. Once the reaction is finished, HCl and zinc powder was cleaned using clean room cotton buds. Patterned substrates were then sequentially cleaned for 20 min each using 10% soap solution (HellmanexTM III) in distilled water, Acetone and Isopropyl Alcohol in an ultrasonicator at room temperature. Gold electrodes were prepared by sputtering unit (Tecport sputtering unit) using shadow mask during sputtering of 10 nm Ti/Ni followed by 100 nm of Gold. Prior to cell fabrication, 20 min UV ozone (Nova Scan PSD- Pro Series) was performed on both FTO and Au electrodes. Cells for mobility measurement were then fabricated by sandwiching 2.5 μm thick mylar sheet in between two electrodes (FTO and Au) at corners with the help of UV curable epoxy to get uniform thickness. The thickness of different samples was measured from the interference maxima and minima in visible to NIR region by recording the transmitted light using Perkin Elmer (Lambda 35) UV-Vis Spectrophotometer. SCLC cells were filled using capillary technique by melting the compounds above (+10 $^{\circ}\text{C}$) their isotropic transition temperature. Once filled, samples were allowed to cool down slowly to the room temperature. Current voltage (J - V) characteristics and dielectric constant ($\epsilon_r = 8.1$ for **1** and **2**) of compound under study was measured using Keithley 4200 SCS Semiconductor Parameter Analyzer.

9.2 Space Charge Limited Current (SCLC) Technique:

Steady State Space Charge Limited current mobility was extracted by recording J - V characteristics on the fabricated sample in which material is sandwiched between injecting (Ohmic/ Au) and non-injecting (non-Ohmic/FTO). A typical J - V characteristics of SCLC measurement is shown in Figure S32 having two distinct regions with slope 1 (Ohmic regime) and slope 2 (SCLC regime), at lower applied voltages the current varies linearly and is represented by Ohm’s law given by equation (a):

$$J = ne\mu \frac{V}{L} \quad (\text{a})$$

Where J is the current density, n is the charge carrier density, e is the elementary charge, μ is the charge carrier mobility (drift), V is the applied voltage and L is the thickness of the SCLC cell used to measure mobility.

Whereas at higher voltages the current is dominated by the injected charges from the contact and J - V characteristics becomes quadratic which can be approximated by Mott-Gurney Equation represented by equation (b):

$$J = \frac{9}{8} \epsilon_r \epsilon_0 \mu \frac{V^2}{L^3} \quad (\text{b})$$

Where ϵ_r is the relative dielectric constant of the material and ϵ_0 (8.854×10^{-12} F/m) is the permittivity of free space. Combining equation (a) and (b) one can calculate the *theoretical threshold voltage* V_T i.e. linear to quadratic switching voltage as:

$$V_T = \frac{8}{9} en \frac{L^2}{\epsilon_r \epsilon_0} \quad (\text{c})$$

The dielectric constant of the material was extracted from their *capacitance-voltage* measurement, is given by equation (d):

$$C = \epsilon_r \epsilon_0 \frac{S}{L} \quad (\text{d})$$

In the equation (d) S is the area of the sample and L is the thickness of the sample.

From the J - V characteristics it is also possible to extract *experimental threshold voltage* (onset of the SCLC regime). Reliability of the measurements can be validated by confronting the *experimental* and *theoretical threshold voltage*.^{9,10} A good agreement between both the values is an indicator of reliable measurement. Alternatively, we also reversed the polarity of the applied voltage (i.e +ve on FTO and -ve on Au electrodes) in order to verify the injection current due to holes. The current observed in this case was always less than that of previous case with no clear SCLC regime.”

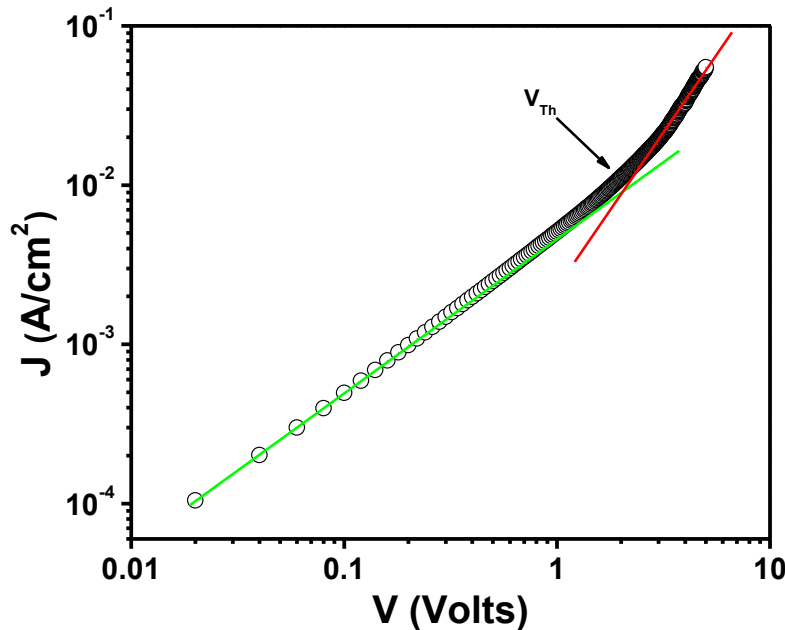


Figure S30. J - V characteristics for compound **1** (at 25 °C) representing ideal Ohmic and SCLC regimes.

We observed a close match (less than 5%) among both experimental as well as theoretical values of threshold voltage (voltage at which current goes from linear to SCLC regime), a broadly acknowledged reliability measure of extracted mobilities in SCLC technique.^{9,10}

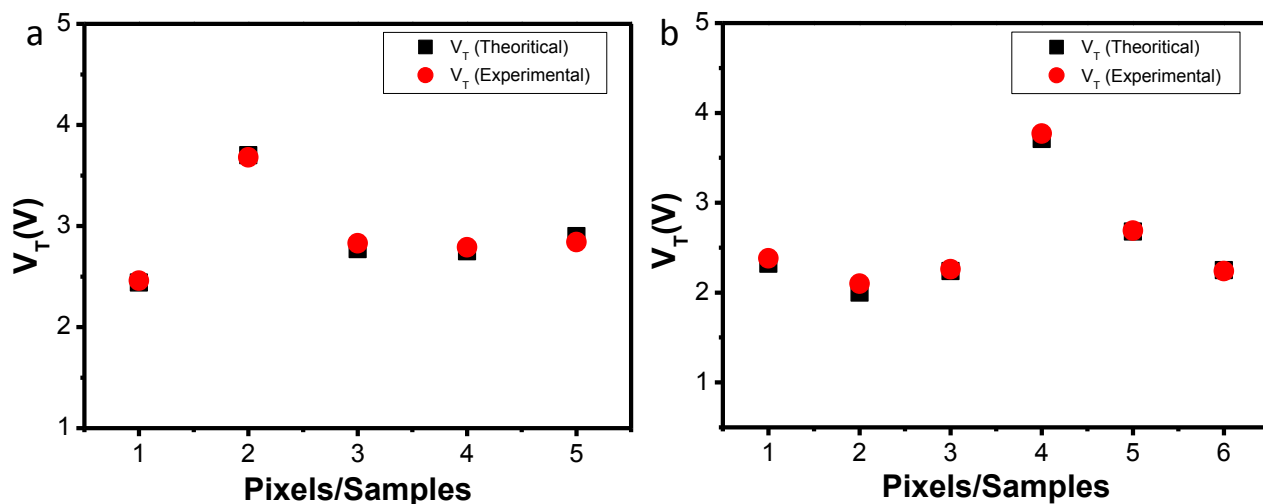


Figure S31. Comparison of theoretical and experimental threshold voltage for (a) hole mobility of 1 and (b) hole mobility of 2.

Table S5. Statistic table of all the mobility values (Hole) for compound 1 and 2.

No of Samples	Compound 1 Mobility (cm ² /V.s)	Compound 2 Mobility (cm ² /V.s)
1	0.05088	4.09177
2	0.04378	3.97574
3	0.03946	1.94538
4	0.04053	3.28056
5	0.03193	3.05663
6	-	4.21982
Average	0.0413	3.42
Std. Dev.	0.0069	0.86
Final	(4.13 ± 0.69) × 10⁻²	3.42 ± 0.86 (4.22)

Table S6. Previous literature reports of highest charge (hole) mobility of thiophene based DLC materials.

S. No.	Journals	Hole Mobility (μ_h) ($\text{cm}^2/\text{V.s}$)
1.	This Report	4.22
2.	<i>J. Am. Chem. Soc.</i> 2013 , <i>135</i> , 18268-18271	2×10^{-2}
3.	<i>J. Am. Chem. Soc.</i> 2011 , <i>133</i> , 13437-13444	1×10^{-3}
4.	<i>J. Mater. Chem. C</i> 2018 , <i>6</i> , 4471-4478	10^{-3}
5.	<i>Chem. Asian J.</i> 2019 , <i>14</i> , 462-470	$10^{-2} - 10^{-3}$
6.	<i>Chem. Asian J.</i> 2009 , <i>4</i> , 1619-1625	5×10^{-4}
7.	<i>ChemPlusChem</i> 2019 , <i>84</i> ,1439-1448	10^{-3}

In general mobility depends on core to core separation and alignment in the mesophase. Even in isotropic phase there may not be complete lack of order and 2D columnar lattice can melt without the complete destruction of columns.¹¹ Therefore the existence of short columns that are correlated on a microscopic scale cannot be ruled out completely in isotropic phase. Such type of short range molecular order in the isotropic phase of nematics are well established in literature.^{12,13} Also in the smectic liquid crystals charge carrier transport (nondispersive) arises in the isotropic phase that are ascribed to originate from the short-range molecular order at that phase.¹⁴ Moreover, the charge mobilities of the same order of magnitude as those observed in columnar phases have also been obtained in nematic discotic (N_D) mesophases in spite of the presence of lower degree of order.¹⁵ Therefore, the same (i.e presence of some order) can be the rationale behind the observed mobility in isotropic phase of compound **2** (refer to Figure 2f in the main manuscript).

10. References

1. I. Bala, W. Y. Yang, S. P. Gupta, J. De, R. A. K. Yadav, D. P. Singh, D. K. Dubey, J. H. Jou, R. Douali and S. K. Pal, *J. Mater. Chem. C*, 2019, **7**, 5724.
2. I. Bala, S. P. Gupta, S. Kumar, H. Singh, J. De, N. Sharma, K. Kailasam and S. K. Pal, *Soft matter*, 2018, **14**, 6342.
3. I. Bala, H. Singh, V. R. Battula, S. P. Gupta, J. De, S. Kumar, K. Kailasam and S. K. Pal, *Chem. Eur. J.*, 2017, **23**, 14718.
4. I. Bala, S. P. Gupta, J. De and S. K. Pal, *Chem. Eur. J.*, 2017, **23**, 12767.
5. J. L. Brusso, O. D. Hirst, A. Dadv and, S. Ganesan, F. Cicoira, C. M. Robertson, R. T. Oakley, F. Rosei and D. F. Perepichka, *Chem. Mater.*, 2008, **20**, 2484.

6. H. Blanco, V. Iguarbe, J. Barberá, J. L. Serrano, A. Elduque and R. Giménez, R., *Chem. Eur. J.* 2016, **22**, 4924.
7. P. Heinz, K. Hindelang, A. Golosova, C. M. Papadakis and B. Rieger, *ChemPhysChem* 2011, **12**, 3591.
8. M. J. Frisch, G. W. Trucks, H. B. Schlegel, G. E. Scuseria, M. A. Robb, J. R. Cheeseman, G. Scalmani, V. Barone, B. Mennucci, G. A. Petersson, H. Nakatsuji, M. Caricato, X. Li, H. P. Hratchian, A. F. Izmaylov, J. Bloino, G. Zheng, J. L. Sonnenberg, M. Hada, M. Ehara, K. Toyota, R. Fukuda, J. Hasegawa, M. Ishida, T. Nakajima, Y. Honda, O. Kitao, H. Nakai, T. Vreven, Jr. J. A. Montgomery, J. E. Peralta,; F. Ogliaro, M. Bearpark, J. J. Heyd, E. Brothers, K. N. Kudin, V. N. Staroverov, R. Kobayashi, J. Normand, K. Raghavachari, A. Rendell, J. C. Burant, S. S. Iyengar, J. Tomasi, M. Cossi, N. Rega, M. J. Millam, M. Klene, J. E. Knox, J. B. Cross, V. Bakken, C. Adamo, J. Jaramillo, R. Gomperts, R. E. Stratmann, O. Yazyev, A. J. Austin, R. Cammi, C. Pomelli, J. W. Ochterski, R. L. Martin, K. Morokuma, V. G. Zakrzewski, G. A. Voth, P. Salvador, J. J. Dannenberg, S. Dapprich, A. D. Daniels, Ö. Farkas, J. B. Foresman, J. V. Ortiz, J. Cioslowski, D. J. Fox, Gaussian 09 (Revision C.01) Gaussian, Inc., Wallingford CT, 2010.
9. J. De, I. Bala, S. P. Gupta, U. K. Pandey and S. K. Pal, *J. Am. Chem. Soc.*, 2019, **141**, 18799.
10. B. Feringan, P. Romero, J. L. Serrano, C. L. Folcia, J. Etxebarria, J. Ortega, R. Termine, A. Golemme, R. Gimenez and T. Sierra, *J. Am. Chem. Soc.*, 2016, **138**, 12511.
11. F. Artzner, M. Veber, M. Clerc and A. M. Levelut, *Liq. Cryst.* 1997, **23**, 27.
12. K. L. Woon, M. P. Aldred, P. Vlachos, G. H. Mehl, T. Stirner, S. M. Kelly and M. O'Neill, *M. Chem. Mater.* 2006, **18**, 2311-2317.
13. P. E. De Gennes, *Phys. Lett.* 1969, **A30**, 454.
14. I. Shiyonovskaya and K. D. Singer, *Phys. Rev. E* 2002, **65**, 041715.
15. A. Concellón, M. Marcos, P. Romero, J. L. Serrano, R. Termine and A. Golemme, *Angew. Chem.* 2017, **129**, 1279.